Biogeosciences, 22, 4649–4677, 2025
https://doi.org/10.5194/bg-22-4649-2025

Biogeosciences Open Access EGU

Land-cover change alters stand structure, species diversity, leaf functional traits, and soil conditions in Cambodian tropical forests

Chansopheaktra Sovann[1,2], Torbern Tagesson[1], Patrik Vestin[1], Sakada Sakhoeun[3], Soben Kim[4], Sothea Kok[2], and Stefan Olin[1]

[1]Department of Physical Geography and Ecosystem Science, Lund University, Sölvegatan 12, 22362 Lund, Sweden
[2]Department of Environmental Science, Royal University of Phnom Penh, Phnom Penh, 120404, Cambodia
[3]Provincial Department of Environment, Ministry of Environment, Siem Reap, 171201, Cambodia
[4]Faculty of Forestry, Royal University of Agriculture, Phnom Penh, 120501, Cambodia

Correspondence: Chansopheaktra Sovann (chansopheaktra.sovann@nateko.lu.se)

Received: 2 December 2024 – Discussion started: 7 January 2025
Revised: 23 May 2025 – Accepted: 25 June 2025 – Published: 15 September 2025

Abstract. Given the severe land-use and land-cover change pressure on tropical forests and the high demand for field observations of ecosystem characteristics, it is crucial to collect such data both in pristine tropical forests and in the converted deforested land-cover classes. To gain insight into the ecosystem characteristics of pristine tropical forests (EFs), regrowth forests (RFs), and cashew plantations (CPs), we established an ecosystem monitoring site in Phnom Kulen National Park, Cambodia. Here, we present the first observed datasets at this site of forest inventories, leaf area index (LAI), leaf traits of woody species, a fraction of intercepted photosynthetically active radiation (fPAR), and soil and meteorological conditions. Using these data, we aimed to assess how land-cover change affects stand structure, species diversity, leaf functional traits, and soil conditions among the three land-cover classes and to evaluate the feasibility of locally calibrated diameters at breast height (DBHs) and tree height (H) allometries for improving aboveground biomass (AGB) estimation. We found significant differences in these ecosystem characteristics, caused by the anthropogenic land-cover conversion, which underlines land-cover change's profound impact on stand structure, species diversity, leaf functional traits, and soil conditions in these tropical forest regions. Our results further demonstrated the feasibility of locally updating aboveground biomass estimates using power-law functions based on relationships between DBH and H. These datasets and findings can contribute to enriching tropical forest research databanks and supporting sustainable forest management.

1 Introduction

Tropical forests cover approximately 14 % of the Earth's surface (Fichtner and Härdtle, 2021) and contribute significantly to global terrestrial biodiversity (Giam, 2017) and biogeochemical cycles (Males et al., 2022). Tropical forests produce at least 30 % of the global terrestrial net primary production (Townsend et al., 2011; Wright, 2013) and account for approximately 70 % of the global gross carbon sink (Pan et al., 2024). In addition, they play a critical role in regulating hydrological cycles on a continental scale (Gloor et al., 2013). Tropical forests have been under severe anthropogenic pressures from agricultural land expansion, resource exploitation (logging, mining), and urbanization (Gardner et al., 2009; Laurance et al., 2014). Such disturbances have resulted in significant structural and functional degradation in tropical forests, highlighting the urgent need to assess how land-cover change alters key ecosystem characteristics (Barlow et al., 2016).

Southeast Asia, though harbouring roughly 15 % of the world's tropical forests (Stibig et al., 2014), has suffered the highest global deforestation rates over the past 15 years (Miettinen et al., 2011). This alarming trend threatens over 40 % of the region's biodiversity by 2100 (Sodhi et al., 2004). The forests are mainly disturbed by timber harvesting (Pearson et al., 2017), slash-and-burn agriculture, and agricultural plantations as a consequence of fulfilling global demands for timber production and agricultural commodities, especially rubber, cashew, oil palm, *Eucalyptus*, and *Acacia* (Phompila et

al., 2014; Grogan et al., 2015; Chen et al., 2016; Johansson et al., 2020). In addition to primary forests, secondary forests that regenerate after clear-cutting or other ecosystem disturbances are also important for protecting biodiversity and assuring the availability of ecosystem services and goods (Tito et al., 2022). While the ecological consequences of forest conversion are broadly recognized, relatively few studies have comprehensively examined how transitions from primary to secondary forests and plantations influence multiple ecosystem characteristics, particularly through detailed field-based observations that may inform our understanding of ecosystem functioning.

Tropical forests demonstrate remarkable ecological complexity, with high diversity in stand structure, species composition, and functional traits shaped by heterogeneous environments and varied disturbance histories (Manuel Villa et al., 2020). This complexity leads to highly site-specific and often inconsistent ecosystem characteristics and responses, making it difficult to generalize the impacts of land-cover change across regions (Wang et al., 2022). A parallel challenge in tropical forest research is the accurate estimation of aboveground biomass (AGB), a key metric for assessing carbon stocks. Most studies rely on generalized allometric models developed under different ecological conditions, assuming similarity in forest structure, composition, and wood density (WD), and these assumptions rarely hold in structurally diverse tropical forests (Vieilledent et al., 2012). These limitations introduce substantial uncertainty when models are applied across sites (Ketterings et al., 2001). The lack of locally calibrated relationships between diameter at breast height (DBH), tree height (H), and wood density and the scarcity of direct destructive sampling further contribute to estimation errors, highlighting the need for site-specific approaches that reflect local variation in forest structure and composition.

In the context of tackling the current challenges of global land-cover change, it is necessary to conduct field observations in order to investigate the responses of ecosystems to changing environmental conditions on fine spatial and temporal scales. Field observations of key ecosystem characteristics, such as forest inventory, leaf functional traits, leaf area index (LAI), fraction of photosynthetically active radiation (fPAR), and soil conditions, provide crucial insights into ecosystem functions and services, including vegetation productivity, carbon sequestration, hydrological cycle, ecosystem stability and resilience to disturbances, nutrient reservoir capacity, and the abundance of habitats of organisms (Naeem et al., 1994; Hector, 1998; Cardinale et al., 2012; Chen et al., 2016; Liang et al., 2016; Parisi et al., 2018; Woodall et al., 2020). In addition, the field data on leaf functional traits, LAI, and fPAR are important for the parameterization and evaluation of remote sensing products and dynamic vegetation models, essential for modelling and upscaling ecosystem responses to anthropogenic disturbances and climate change (Feng et al., 2018; Fang et al., 2019; Pei et al., 2022). Recognizing the significant role and high demand for field observations of ecosystem characteristics, open data repositories, such as FLUXNET, ICOS Carbon Portal, SpecNet, and the TRY database, have been established to facilitate data sharing (Gamon et al., 2010; Kattge et al., 2020; Pastorello et al., 2020). Despite those global initiatives, observed data from tropical forests that support multi-class, pairwise comparisons for capturing ecosystem changes across gradients of forest degradation and land-use conversion remain limited. This gap is especially critical in Southeast Asia, where rapid forest-to-agriculture transitions threaten key ecosystem functions, and understanding these ecosystem changes is essential for informing evidence-based conservation and restoration strategies (Fan et al., 2024).

Within this context, Phnom Kulen National Park (Kulen) in Cambodia emerges as a critical landscape for investigating ecosystem responses to land-cover change. Kulen is a hotspot for ecosystem service provisioning in Cambodia, mainly for water supply, potential carbon sink, and cultural services (Jacobson et al., 2022; Kim et al., 2023). It is the origin of the Khmer Empire and contains numerous archaeological sites. The stream water from the mountain is not only used to support local livelihoods in water supply and irrigation downstream (Somaly et al., 2020), but it is also the primary water source to recharge surface-water and groundwater aquifers in Angkor Wat, a UNESCO World Heritage Site. Hence, the area is of high importance to ensure that the temples' foundations remain stable and maintain their surrounding forest ecosystem (Hang et al., 2016). However, previous studies revealed that the forestland in and around Kulen has been disturbed, largely driven by agricultural expansion, particularly the spread of cashew plantations (CPs) (Chim et al., 2019; Sovann et al., 2025).

Given increasing concerns about land-use and land-cover change threatening the high-value ecosystem functions of tropical forests such as those in Kulen, our study aims to gain insight into the impact of land-cover conversion on key ecosystem characteristics. Specifically, our first objective is to assess the differences in stand structure, species diversity, leaf functional traits, and soil conditions between pristine tropical forests and the land cover into which the deforested regions are converted (regrowth forests and cashew plantations). We hypothesize that there will be a reduction in stand structural complexity, species composition, and leaf functional traits and a marked change in soil conditions. Additionally, our second objective is to evaluate the feasibility of locally updating aboveground biomass estimates by applying power-law functions derived from site-specific relationships between diameter at breast height and tree height, with the hypothesis that locally calibrated DBH–H relationships will have a substantial effect on estimated aboveground biomass compared to regional or generalized allometric models. To test these hypotheses, we will analyse a novel in situ dataset collected from pristine tropical forests, regrowth forests, and

cashew plantations at a newly established ecosystem monitoring site in Phnom Kulen National Park, Cambodia.

2 Materials and methods

2.1 Study area and selection of plots

The selected study area is the Phnom Kulen National Park located in the Siem Reap Province in northwestern Cambodia (Fig. 1). It covers 37 380 ha predominantly on Jurassic–Cretaceous sandstone plateaus, and the highest peak is 496 m (Matschullat, 2014; Geissler et al., 2019). In 2021, 72 % of Phnom Kulen National Park was forested, dominated by nearly intact tropical evergreen forests (EFs) (30 %) and forests that regrow naturally after clear-cutting (RFs) (7 %). The remaining 35 % of forest cover consisted of semi-evergreen, deciduous, and bamboo stands. Non-forest areas were dominated by household-scale cashew plantations (CPs) (15 %), with the remaining 13 % consisting of croplands, paddy fields, settlements, and tree and rubber plantations (Sovann et al., 2025).

Nine forest inventory plots were established in Kulen in December 2020, three within each of the EF, RF, and CP land-cover classes (Fig. 1, Table 1, Fig. S1), with a minimum separation of 250 m to capture stand structure variation for each land-cover class. The EF plots represented tropical evergreen forests with no clear-cut history. The RF plots were dominated by at least 10-year-old natural regrowth forests, and RF1 was clear-cut in 2009, while RF2 and RF3 experienced timber harvesting, burning, and fuelwood collection from 2006 to 2013. The CP plots were permanent rainfed cashew plantations, with cashew trees planted in 2013 in CP1 and in 2012 in CP2 and CP3.

2.2 Data collection

2.2.1 Forest inventory

The forest inventory was performed by following the standard method of the National Forest Inventory of Cambodia (Than et al., 2018). Each plot was designed as a rectangle with 50 m × 30 m long edges in the south–north and west–east directions. The plots were further subdivided into five subplots with the following dimensions: 2 m × 2 m, 5 m × 5 m, 10 m × 10 m, 30 m × 15 m, and 30 m × 50 m (Fig. S2). In the 2 m × 2 m subplots, seedlings with diameters at breast height (1.3 m above ground level, a.g.l.) of less than 1 cm were recorded. In the 5 m × 5 m, 10 m × 10 m, 30 m × 15 m, and 30 m × 50 m subplots, trees with DBH ranges of 1–5, 5–15, 15–30, and greater than 30 cm were measured, respectively.

For seedlings, we only recorded the total numbers of each species. For the DBH range of 1–5 cm, we noted the DBH, tree height, species, local name (Khmer), and position of each tree. For trees with a DBH greater than 5 cm, we collected the same data as for trees with a DBH of 1–5 cm, plus bole height (the height from the ground to the first main lowest stem), health (healthy or infected), quality (straight, bent, or crooked stem), origin (natural or planted), and stump diameter and height (measured 15 cm a.g.l. for annual tree growth monitoring).

Deadwood is a significant indicator of decomposition and nutrient cycling processes in a forest ecosystem (Shannon et al., 2021). Data on lying and standing deadwood with a DBH greater than 10 cm in the 30 m × 15 m subplots were also collected. The deadwood decomposition levels were classified into five scales, based on harmonizing the scaling systems of the National Forest Inventory of Sweden (Swedish University of Agricultural Sciences, 2021) and Cambodia (Than et al., 2018) (Table S1). For standing deadwood, we recorded the species, local name, location, height, and decomposition level. For lying deadwood, we counted the number of pieces and measured the lengths, base and tree diameters, and decomposition levels.

2.2.2 Leaf sample collection and measurement

A total of 453 leaf samples from 30 woody species were collected inside and 500 m around the forest inventory plots in December 2019 and August 2022. Each species was represented by 5 to 47 leaf samples. Each leaf's fresh mass, chlorophyll content, and photo were taken in the field. A chlorophyll meter (SPAD 502 Plus; Konica Minolta Sensing Inc., Japan) was used in situ to measure chlorophyll content five times on each leaf surface to retrieve a leaf mean value. The given measurement unit was in Soil Plant Analysis Development (SPAD) value and later converted to chlorophyll (Chl) a and b content in $\mu g\,cm^{-2}$ (Coste et al., 2010). We obtained fresh leaf mass by weighting in the field and leaf dry mass by oven-drying the leaves at 60 °C until the leaf mass remained constant (oven-dried for at least 3 d) (Garnier et al., 2001). The leaf photos were used for estimating leaf lengths and areas using ImageJ (Schindelin et al., 2012; Schneider et al., 2012).

2.2.3 Meteorological and photosynthetically active radiation data

A meteorological station was installed in an open area to continuously record meteorological conditions and incoming photosynthetically active radiation (PAR) for the wider area (the Kulen National Park). Data were sampled at 1 min intervals and stored as 15 min averages (sum for rainfall). The installation was done in November 2020 in Khnang Phnom Commune, Svay Luer District, Siem Reap Province, at an altitude of 314 m above mean sea level and at 13°34′16.1148″ N, 104°9′45.6768″ E. The station has one Atmos 41 meteorological station (Meter Group Inc. WA, USA), installed 2.2 m a.g.l., measuring rainfall, wind speed, wind direction, global radiation, atmospheric pressure, and

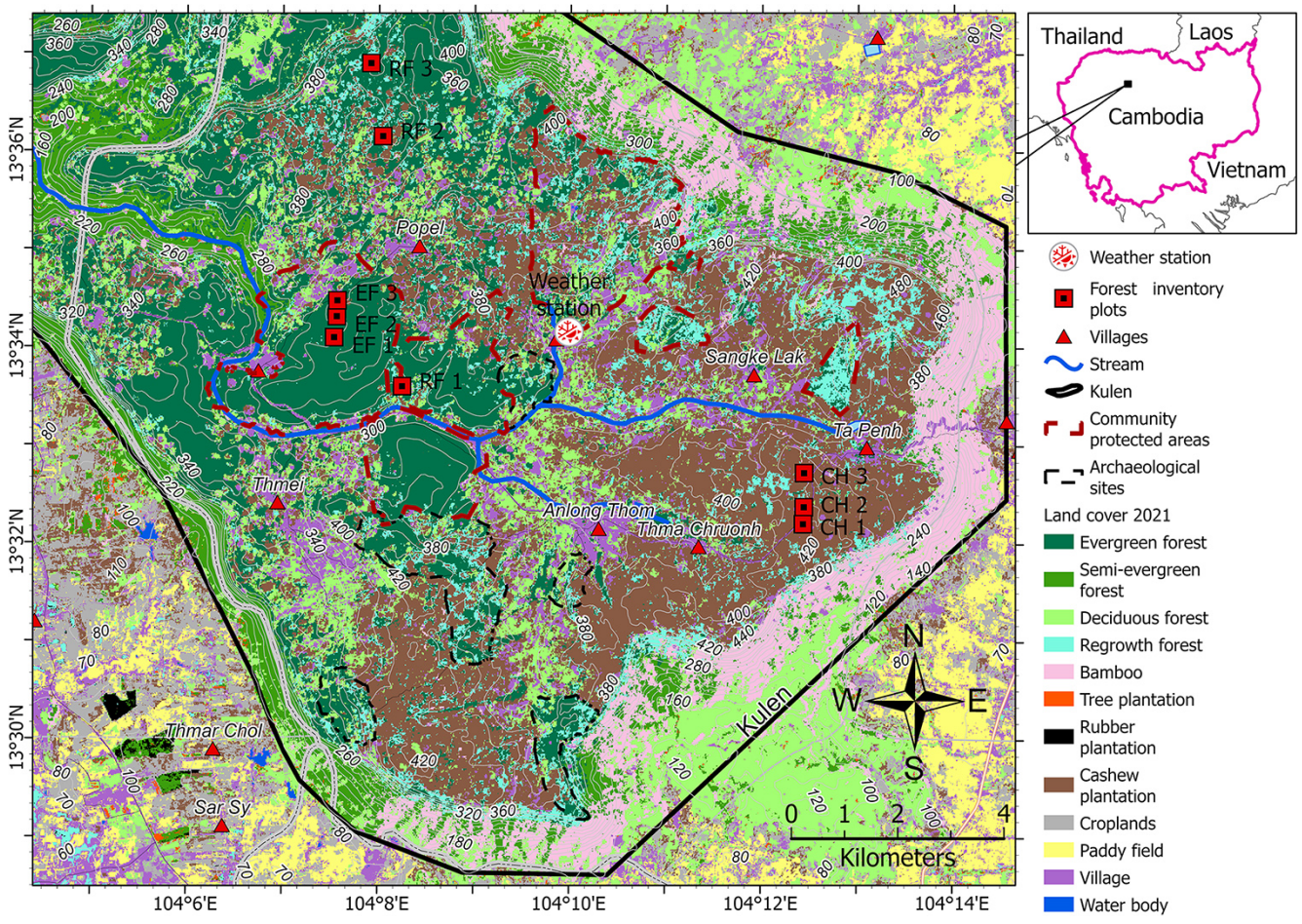

Figure 1. The locations of the nine forest inventory plots and the meteorological station in the Phnom Kulen National Park, Cambodia. Note: the background land cover 2021 was derived from Sovann et al. (2025).

air temperature. Additionally, four PAR sensors (SQ-110-SS, Apogee Instruments, Inc., UT, USA) were positioned 2 m a.g.l. to record incoming PAR (PAR_{inc}) (Fig. S3).

Six additional loggers with five PAR sensors (SQ-521-SS and SQ-110-SS, Apogee Instruments, Inc., UT, USA) and one TEROS 12 soil moisture sensor each (Meter Group Inc. WA, USA), collecting data at a 15 min mean time step, were installed in six of the forest inventory plots in April 2022. The soil moisture sensors were installed at a depth of 20 cm to measure soil water content (SWC), soil temperature (Ts), and soil electrical conductivity (ECs). Two loggers were placed in each land-cover class (EF, RF, and CP). The selection of plots in each land-cover class was based on previous measurements of leaf area index, and the loggers were placed at the plots with the highest and lowest LAI for each land cover, respectively. Thus, the selected plots for installing PAR sensors were EF1, EF3, RF1, RF3, CP2, and CP3 (Fig. 1). One PAR sensor was placed in the centre of the plot, and the other four were placed 15 ± 1 m apart at 30, 150, 220, and 330° from the north. In cases of unfavourable field conditions, such as high termite nests or being too close to a tree, the locations were adjusted 0.5–1 m east or west of the planned position. Each PAR sensor was mounted on 1.3 m poles to record PAR below-canopy data. We calculated the fraction of PAR intercepted by the stand canopy for each plot using Eq. (1) (Olofsson and Eklundh, 2007). Each TEROS 12 soil moisture sensor was installed at a depth of 20 cm in the middle of the six plots to measure SWC, Ts, and ECs. The data of fPAR and soil conditions from two plots within the same land-cover classes were averaged to represent those classes.

$$\mathrm{fPAR} = \frac{(\mathrm{PAR_{inc}} - \mathrm{PAR_{below}})}{\mathrm{PAR_{inc}}}, \quad (1)$$

where PAR_{inc} and PAR_{below} are photosynthetically active radiation above and below canopy ($\mu mol\ m^{-2}\ s^{-1}$) and fPAR is a percentage.

2.2.4 Leaf area index measurements

We measured each plot's total one-sided leaf surface area per unit ground area, LAI, using an LAI-2000 Plant Canopy An-

Table 1. Characteristics of the forest inventory plots in Phnom Kulen National Park. Note: EF = evergreen forest; RF = regrowth forest; and CP = cashew plantation. Data source: soil type and geology data from Matschullat (2014). Disturbance history information is obtained from field observation, from discussion with local people, and by combining the Global Forest Change dataset of Hansen et al. (2013) with the LandTrendr Pixel Time Series Plotter tool of Kennedy et al. (2018).

Plot ID	Latitude, longitude	Elevation (m)	Soil type	Disturbance history
EF1	13°34′12.4680″ N 104°7′18.6096″ E	331	Acid lithosols	No clear-cut history; affected by wind disturbance and human collection of wild honey, lychee, and other wild fruits in 2006, 2012, and 2014. Fewer large tree stands and lower vegetation cover density compared to EF2 and EF3.
EF2	13°34′25.3452″ N 104°7′20.2872″ E	349	Acid lithosols	No clear-cut history; past disturbances include cutting one lychee tree for fruit harvesting in 2022.
EF3	13°34′35.0508″ N 104°7′20.6148″ E	339	Acid lithosols	No clear-cut history; a wind-driven disturbance occurred in 2023.
RF1	13°33′42.6132″ N 104°8′1.2408″ E	331	Red-yellow podzols	Evergreen forest clear-cut in 2009.
RF2	13°36′15.6924″ N 104°7′48.8928″ E	371	Acid lithosols	Timber harvesting, burning, and fuelwood collection of an evergreen forest from 2006 to 2013.
RF3	13°37′0.3612″ N 104°7′41.358″ E	401	Acid lithosols	Timber harvesting, burning, and fuelwood collection of an evergreen forest from 2006 to 2013.
CP1	13°32′18.8988″ N 104°12′12.5568″ E	429	Red-yellow podzols	Cashew plantation established in 2013.
CP2	13°32′29.3100″ N 104°12′13.0284″ E	422	Red-yellow podzols	Cashew plantation established in 2012.
CP3	13°32′50.1864″ N 104°12′13.1544″ E	430	Red-yellow podzols	Cashew plantation established in 2012.

alyzer (LI-COR, NE, USA). The measurements were conducted six times across two seasons: four times during the dry season (November/December 2019, November 2020, December 2020, and March 2021) and twice during the rainy season (September 2020 and June 2021). The measurements were taken both at ground level to capture the total LAI (LAI_T) and at breast height to specifically assess tree canopy LAI (LAI_C) within two diagonal transects across the 50 m × 30 m rectangular plots. On each measurement occasion, we collected between 32 and 75 samples, except for the ground-level measurements of the RF3 plot in December 2020, where only 10 samples were collected due to technical issues.

2.3 Data analysis

2.3.1 Species diversity

We investigated the species diversity of various land covers by calculating species richness (S_R) and the Shannon–Wiener index (S_H) (Shannon, 1948). The S_R was determined by summing the number of tree species in each plot. The S_H is commonly used to quantify species richness and evenness in a community by representing the number of species and how equally individuals are distributed among them (Hill, 1973). The value of S_H increases as the number of species and the degree of evenness increase. The S_H was calculated as follows:

$$S_H = -\sum_{i=1}^{n} P_i \ln(P_i), \quad (2)$$

where S_H is the Shannon–Wiener index (unitless), P_i is a proportion of i species in a community (unitless), and n is the number of species in a plot (unitless). We calculated the S_R and S_H at the plot level and then averaged the values for each land-cover class.

2.3.2 Functional traits and diversity

We computed the specific leaf area (SLA) for each of the 453 leaf samples as the ratio of leaf area to leaf dry mass. Likewise, leaf dry matter content (LDMC) was calculated by the ratio of dry leaf mass to fresh leaf mass (Garnier et al., 2001; Akram et al., 2023). We estimated the trait community-weighted means and standard deviations of SLA_{cwm}, $LDMC_{cwm}$, and Chl_{cwm} to represent ecosystem

functions and their diversity at the land-cover level (Garnier et al., 2004; Leoni et al., 2009; Wang et al., 2020) as follows:

$$T_{\mathrm{cwm}} = \frac{\sum_{i=1}^{n} W_i T_i}{\sum_{i=1}^{n} W_i}, \tag{3}$$

where T_{cwm} is the trait community-weighted mean for SLA, LDMC, or Chl; T_i is the species-specific trait value tree i; n is the total number of trees; and W_i is the weight (volume-based) value of the tree, assuming that larger trees have a greater impact on the ecosystem function (Chave et al., 2005; Feldpausch et al., 2011). Before computing T_{cwm} for each trait, we addressed missing species traits within each plot by firstly taking values from a different plot with the same land-cover class. If unavailable, we used values from the same species across all nine plots, followed by values from the genus and family levels. When multiple genera or families were available, we averaged the values. If neither was available, we used the mean trait value of the plot.

2.3.3 Stand structural attributes

We examined the differences in DBH, H, basal area (BA), aboveground biomass, and deadwood biomass (DWB) for the various land-cover classes to characterize stand structure attributes. Deadwood volumes (V_{DW}, m^3) for each bole were determined by Smalian's equation:

$$V_{\mathrm{DW}} = (\pi\ H_b)\ \frac{\left(D_{\mathrm{base}}^2 + D_{\mathrm{top}}^2\right)}{8}, \tag{4}$$

where D_{base} and D_{top} are diameters at base and top (m) and H_b is the length/height of the trunk (m).

Deadwood biomass was then received by multiplying V_{DW} with a mean deadwood density of $0.45\,\mathrm{g\,cm^{-3}}$ (Kiyono et al., 2007). Total DWB was computed plot-wise by taking the sum of lying and standing DWB. DWB for each land-cover class was calculated as the average of the total DWB across the plots within that land-cover class.

Basal area was determined plot-wise by combining the DBH of all living trees within a plot:

$$\mathrm{BA} = \sum_{i=1}^{n} \pi \left(\frac{\mathrm{DBH}_i}{2}\right)^2 \left(\frac{10^4}{A_i}\right), \tag{5}$$

where BA is the plot-wise total basal area of all living trees ($\mathrm{m^2\,ha^{-1}}$), n is the number of trees in a plot, DBH_i is the diameter at breast height of tree i in a sampling plot (m), $\pi\left(\frac{\mathrm{DBH}_i}{2}\right)^2$ is the circle basal area of tree i ($\mathrm{m^2}$), and $\left(\frac{10^4}{A_i}\right)$ is the scaling factors employed to convert the sampled subplot area (A_i) to 1 ha (unitless). The BA for each land-cover class was represented by the mean BA of all plots within a class.

We calculated the mean and standard deviation of DBH and H for each plot and land cover. We further used these for establishing relationships between DBH and H, as such relationships serve as functional traits characterizing tree growth patterns and successional stages within forest communities (Nyirambangutse et al., 2017; Howell et al., 2022). We used natural logarithms and then converted them to power-law relationships according to both plot- and land-cover class (West and Brown, 2005). An ordinary least-squares (OLS) linear regression was applied to investigate the DBH–H relationship, followed by transforming the relationship into a power-law relationship (Huxley, 1932).

$$H = K_1 \mathrm{DBH}^{K_2}, \tag{6}$$

where K_1 and K_2 are the power-law intercept and slope, respectively. The K_1 captures the overall scaling relationship between H (m) relative to DBH (cm) within a forest community, while K_2 regulates the rate of H increase relative to DBH growth.

The obtained K_1 and K_2 values were further used to estimate AGB ($\mathrm{AGB_h}$) Eq. (7) in Table 2. We also computed the AGB using existing equations (Table 2, Eqs. 9–11) ($\mathrm{AGB_f}$) adopted for the three different land-cover classes. These EF and RF allometric equations were developed for tropical multiple species, whereas the CP equation was a species-specific allometric equation for the cashew tree (Malimbwi et al., 2016). The wood density values required for the AGB estimations were species-specific and obtained from The International Council for Research in Agroforestry (ICRAF, 2022) and Zanne et al. (2009). When multiple WD values for a tree species were available, the mean value was used, whereas, when no species-specific WD values were available, the average of tropical Asia ($0.57\,\mathrm{g\,cm^{-3}}$) was used (Reyes et al., 1992). The applied WD values for this study then ranged from 0.39–$1.04\,\mathrm{g\,cm^{-3}}$. Specifically, the WD values (mean $\pm$ 1 standard deviation) for EFs, RFs, and CPs were 0.74 ± 0.17, 0.72 ± 0.15, and $0.45\,\mathrm{g\,cm^{-3}}$, respectively. We first estimated AGB at the plot level in kilograms, then scaled these values to megagrams per hectare, and then averaged per land-cover class.

2.3.4 Statistical analysis

Descriptive statistics were conducted to examine the difference in ecosystem characteristics between plots and land-cover classes. One-way ANOVA tests (ANOVA) were used to assess significant differences in mean values across land-cover classes. Tukey's honestly significant difference test (Tukey HSD) was further employed for pairwise comparisons between land-cover classes. Pearson correlation and ordinary least-squares regression analyses were used to explore relationships between variables. All analyses were performed using R 4.2.3 (R Core Team, 2023).

Table 2. Allometric equations used for estimating aboveground biomass (AGB; kg per tree) in the different land-cover classes.

No.	Equation	Land cover	AGB allometric equation	Regions	n	DBH (range, cm)	$\overline{WD_f}$ (mean ± SD, g cm^{-3})	References
1	Eq. (7)	All	$AGB_h = \frac{WD\,\pi\,K_1}{8}\,DBH^{2+K_2} + \varepsilon$	–	–	–	–	This study
2	Eq. (8)	All	$AGB_{wd} = \frac{WD}{\overline{WD_f}}\,AGB_f$	–	–	–	–	This study
3	Eq. (9)	EF	$AGB_f = 0.1184\,DBH^{2.53}$	Pantropical	170	5.0–148.0	0.58 ± 0.02	Brown (1997)
4	Eq. (10)	RF	$AGB_f = 0.0829\,DBH^{2.43}$	Sarawak, Malaysia	136	0.1–28.7	0.38 ± 0.07	Kenzo et al. (2009)
5	Eq. (11)	CP	$AGB_f = 0.8450\,DBH^{1.77}$	Pwani, Tanzania	45	6.0–89.9	0.18	Malimbwi et al. (2016), Mlagalila (2016)

Note: EF is evergreen forest, RF is regrowth forest, and CP is cashew plantation. In Eqs. (9)–(11), DBH is the diameter at breast height (cm), and $\overline{WD_f}$ is the reported mean wood density used in AGB_f (kg m^{-3}). In Eq. (7), K_1 and K_2 are derived power-law intercept and slope values between the DBH (cm) and tree height (H, m) relationship in Eq. (6), ε is a statistical error term, WD is wood density for each tree species (g cm^{-3}), and DBH is in centimetres. In this study, in Eq. (7), we employed a trunk shape factor of 1/8 for calculating the volume of frustum cones, as proposed by King et al. (2006). This factor falls within the range of 1/4 (cylinder volumes) to 1/12 (cone volumes). In Eq. (8), AGB_{wd} is our examined aboveground biomass based on Eqs. (9)–(11) with species-specific wood density updated for our woody tree species, and WD is the species-specific wood density of trees in each plot (g cm^{-3}).

3 Results

3.1 Meteorological and soil conditions

The observed annual daily mean air temperature from April 2022 to April 2023 at Kulen meteorological station was 24.2 ± 2.0 °C, varying between 17.8 and 28.6 °C (Fig. 2a). The total annual rainfall was 2290 mm, significantly surpassing nearby lowland stations: Banteay Srei station, located 22 km west, recorded 1160 mm, and Siem Reap City station, situated 40 km southwest, recorded 1475 mm (Chim et al., 2021). About 90 % of the annual precipitation fell during the rainy season from May to November, with September being the wettest month (505 mm). The daily maximum rainfall can reach up to 141 mm, but the daily mean during the rainy season was 11.2 ± 19.7 mm (Fig. 2b). The annual daily mean of global radiation, relative humidity, vapour pressure deficit, and wind speed were 172 ± 44 W m^{-2}, 88 ± 12 %, 0.45 ± 0.21 kPa, and 0.68 ± 0.22 m s^{-1}, respectively (Fig. 2c–f).

Soil conditions varied significantly among land-cover classes (ANOVA and Tukey HSD, p value < 0.001). Annual daily mean soil temperature was highest in CPs (25.8 °C), exceeding values in EFs (24.3 °C) and RFs (24.2 °C). In contrast, annual daily mean soil water content was lowest in RFs (0.14 m^3 m^{-3}) compared to EFs (0.23 m^3 m^{-3}) and CPs (0.21 m^3 m^{-3}) (Table 3). Annual daily mean soil electrical conductivity was highest in EFs (0.039 dS m^{-1}), followed by RFs (0.032 dS m^{-1}) and CPs (0.025 dS m^{-1}). Overall, daily mean values across land-cover classes ranged between 0.14–0.23 m^3 m^{-3} for SWC, 24.2–25.8 °C for Ts, and 0.025–0.039 dS m^{-1} for ECs (measured at 20 cm depth; Fig. 2g–i).

3.2 Species diversity

A total of 343 observations (292 trees and 51 seedlings) from 47 woody species (including 13 seedling species) and 32 families (including 7 seedling families) were identified from the nine plots (Table S3). No statistical test of significance of differences in species diversity among land-cover classes was possible due to too few sampled plots. However, species diversity declined markedly from evergreen forests to regrowth forests and was lowest in cashew plantations, as reflected in both species richness and the Shannon–Wiener index. The average S_R per plot was 17 in EFs, 13 in RFs, and only 4 in CPs. Similarly, the S_H was highest in EFs (2.48 ± 0.33), intermediate in RFs (1.97 ± 0.45), and lowest in CPs (0.61 ± 0.46), with individual plot values ranging from 0.31 (CP2) to 2.68 (EF1) (Table S4). Species composition was more evenly distributed in EFs and RFs but naturally strongly dominated by a single species in CPs. In EFs, the top five most abundant species, *Mesua ferrea* ($n = 18$), *Diospyros bejaudii* ($n = 12$), *Litchi chinensis* ($n = 11$), *Vatica odorata* ($n = 11$), and *Hydnocarpus annamensis* ($n = 8$), accounted for 46 % of the individuals. In RFs, *Vatica odorata* ($n = 54$), *Nephelium hypoleucum* ($n = 14$), *Benkara fasciculata* ($n = 12$), *Garcinia oliveri* ($n = 12$), and *Mesua ferrea* ($n = 5$) made up 61 %. In contrast, CPs were dominated by *Anacardium occidentale* ($n = 46$), which was the only tree species observed excluding seedlings. Additional seedling species in CPs included *Strychnos axillaris* ($n = 3$), *Nephelium hypoleucum* ($n = 1$), *Melodorum fruticosum* ($n = 1$), *Maclura cochinchinensis* ($n = 1$), and *Catunaregam tomentosa* ($n = 1$). Furthermore, fast-growth species, as described by Ha (2015) (WD < 0.6 g cm^{-3}), accounted for 40 % of EFs and 44 % of RFs of their total species composition.

3.3 Leaf functional traits

At the species level, the mean specific leaf area for all 30 species was 16.97 ± 5.30 m^2 kg^{-1}, with *Hydnocarpus annamensis* having the highest SLA (36.67 ± 5.20 m^2 kg^{-1}) and *Capparis micracantha* having the lowest (10.46 ± 3.28 m^2 kg^{-1}). For Chl, the mean value was 10.28 ± 4.17 mg g^{-1}, with *Hydnocarpus annamensis* having the highest value (25.75 ± 5.28 mg g^{-1}) and *Anacardium occidentale* having the lowest (4.86 ± 4.93 mg g^{-1}). Finally, for LDMC, the mean value was 378.96 ± 143.26 mg g^{-1},

https://doi.org/10.5194/bg-22-4649-2025

Table 3. Mean values and statistics of ecosystem characteristics in the different land-cover classes.

Group	Variables	Land cover						ANOVA	Tukey HSD		
		EF (mean ± SD)	*n*	RF (mean ± SD)	*n*	CP (mean ± SD)	*n*	*p* value	EF and CP *p* value	EF and RF *p* value	RF and CP *p* value
Species diversity	S_R (with seedling species, count per plot)	17 ± 4	3	13 ± 2	3	4 ± 3	3	–	–	–	–
	S_R (without seedling species, count per plot)	13 ± 2	3	10 ± 3	3	1 ± 0	3	–	–	–	–
	S_H (with seedling species, unitless)	2.48 ± 0.33	3	1.97 ± 0.45	3	0.61 ± 0.46	3	–	–	–	–
Leaf functional traits	Chl_{cwm} (mg g^{-1})	9.14 ± 3.45	109	7.56 ± 2.03	137	4.99 ± 0.66	46	*	*	0.39	0.08
	$LDMC_{cwm}$ (mg g^{-1})	398.43 ± 72.24	109	370.13 ± 94.97	137	407.64 ± 21.68	46	0.51	0.50	0.94	0.69
	SLA_{cwm} (m^2 kg^{-1})	18.18 ± 2.86	109	14.87 ± 2.06	137	11.99 ± 1.45	46	**	**	*	0.06
Stand structure	DBH (cm)	18.0 ± 20.1	109	5.8 ± 4.3	137	13.0 ± 3.9	46	***	0.14	***	***
	H (m)	17.0 ± 13.3	109	7.4 ± 3.8	137	6.3 ± 1.0	46	***	***	***	0.93
	Maximum H (m)	52.0	109	18.6	137	7.8	46	–	–	–	–
	Wood density (g cm^{-3})[a]	0.74 ± 0.17	109	0.72 ± 0.15	137	0.45 ± 0.00	46	***	***	0.56	***
	Stem density DBH > 1 cm (ha^{-1})[b]	6216 ± 2177	3	10859 ± 4999	3	1067 ± 440	3	–	–	–	–
	Stem density DBH > 5 cm (ha^{-1})[b]	1016 ± 533	3	2193 ± 895	3	1067 ± 440	3	–	–	–	–
	Stem density DBH ≥ 10 cm (ha^{-1})[b]	550 ± 505	3	293 ± 6	3	600 ± 164	3	–	–	–	–
	BA (m^2 ha^{-1})	26.2 ± 3.6	3	17.0 ± 5.4	3	11.6 ± 3.5	3	–	–	–	–
	BA (m^2 ha^{-1}, DBH ≥ 5 cm)	23.7 ± 4.4	3	11.6 ± 2.4	3	11.6 ± 3.5	3	–	–	–	–
	BA (m^2 ha^{-1}, DBH ≥ 10 cm)	21.1 ± 4.4	3	4.4 ± 0.7	3	9.2 ± 1.8	3	–	–	–	–
	DWB (total) (Mg ha^{-1})	27.5 ± 12.4	3	4.8 ± 7.0	3	0.4 ± 0.2	3	–	–	–	–
	AGB_f (Mg ha^{-1})	239 ± 92	3	42 ± 10	3	71 ± 22	3	–	–	–	–
	AGB_{wd} (Mg ha^{-1})	336 ± 168	3	78 ± 25	3	182 ± 57	3	–	–	–	–
	AGB_h (Mg ha^{-1})	312 ± 184	3	54 ± 14	3	17 ± 5	3	–	–	–	–
	LAI_C (m^2 m^{-2})	4.62 ± 0.50	21	4.66 ± 0.70	21	2.52 ± 0.42	21	***	***	1.00	***
	LAI_T (m^2 m^{-2})	6.16 ± 0.67	21	5.57 ± 0.76	21	3.07 ± 0.61	21	***	***	0.08	***
	Annual mean fPAR[c]	0.97 ± 0.01	364	0.96 ± 0.01	365	0.76 ± 0.06	359	***	***	*	***
Soil conditions	Annual mean SWC[c] (m^3 m^{-3})	0.23 ± 0.06	364	0.14 ± 0.03	365	0.21 ± 0.05	363	***	***	***	***
	Annual mean Ts[c] (°C)	24.3 ± 1.2	364	24.2 ± 1.3	365	25.8 ± 1.5	363	***	***	***	***
	Annual mean ECs[c] (dS m^{-1})	0.039 ± 0.015	268	0.032 ± 0.013	40	0.025 ± 0.003	260	***	***	***	***

Abbreviations used in the table: EF = evergreen forest; RF = regrowth forest; CP = cashew plantation; S_R = species richness (only woody seedling species); S_H = Shannon–Wiener index; Chl_{cwm} = community-weighted mean of chlorophyll *a* and *b* content; $LDMC_{cwm}$ = community-weighted mean of leaf dry matter content; SLA_{cwm} = community-weighted mean of specific leaf area; DBH = tree's diameter at breast height; H = tree height; BA = stand basal area; AGB_f = aboveground biomass computed by adopted functions; AGB_h = aboveground biomass computed by H and DBH power-law relationship; AGB_{wd} = aboveground biomass based on Eqs. (9)–(11) with species-specific wood density updated for our woody tree species; LAI_C = canopy leaf area index; LAI_T = total leaf area index; fPAR = fraction of photosynthetically active radiation; SWC = soil water content; Ts = soil temperature; ECs = soil saturation extract electrical conductivity; SD = standard deviation; ANOVA = one-way analysis of variance; Tukey HSD = Tukey's honestly significant difference test. Statistically significant code for ANOVA and Tukey HSD test: "***" *p* value < 0.001, "**" *p* value < 0.01, "*" *p* value < 0.05, and "–" not available. [a] The species-specific wood density was derived from the ICRAF (2022) and Zanne et al. (2009). [b] Extrapolated values for 1 ha were obtained from sampling DBH class subplots. [c] Daily mean values were used to calculate the reported variables.

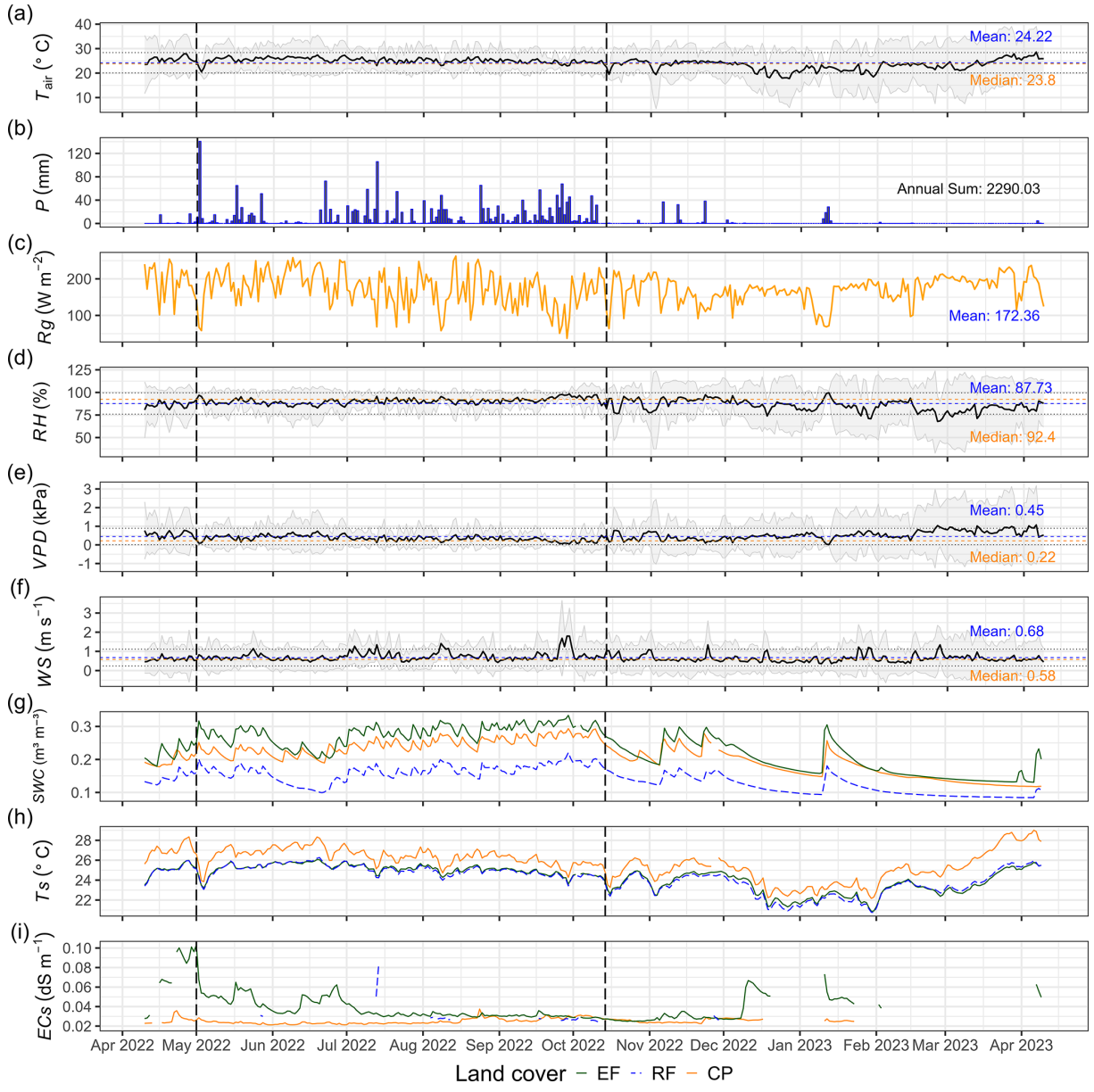

Figure 2. The meteorological conditions at Kulen meteorological station **(a–f)** and soil conditions at each land-cover class **(g–i)** from 10 April 2022 to 9 April 2023. **(a)** Daily mean air temperature (T_{air}; °C), **(b)** daily total precipitation (P; mm), **(c)** daily mean global radiation (Rg; W m^{-2}), **(d)** daily mean relative humidity (RH; %), **(e)** daily mean vapour pressure deficit (VPD; kPa), **(f)** daily mean wind speed (WS; m s^{-1}), **(g)** daily mean soil water content (SWC; m^3 m^{-3}), **(h)** daily mean soil temperature (Ts; °C), and **(i)** daily mean soil saturation extraction electrical conductivity (ECs; dS m^{-1}). The vertical dashed lines in each plot highlight the rainy season in Cambodia from May to October. The grey-shaded regions around the mean in panels **(a)**, **(d)**, **(e)**, and **(f)** represent the 95 % confidence interval (using 1 standard deviation) from the daily mean, while the blue horizontal dashed line represents the yearly mean, the brown horizontal dashed line represents the yearly median, and the black horizontal dotted line represents a yearly standard deviation (see Table S2 and Fig. S4, which present Kulen meteorological station's annual and monthly meteorological data. Figures S5–S7 show monthly mean soil conditions by land-cover class, and Fig. S8 depicts correlations between meteorological and soil conditions).

with *Mesua ferrea* and *Hydnocarpus annamensis* having the highest (486.90 ± 25.03 mg g^{-1}) and lowest (139.92 ± 20.19 mg g^{-1}) values, respectively. For detailed descriptions of leaf functional traits of all species and plots, please refer to Tables S5–S7.

Across land-cover classes, mean SLA_{cwm} and Chl_{cwm} decreased from EFs to RFs to CPs. SLA_{cwm} and Chl_{cwm} were highest in EFs (18.18 ± 2.86 m^2 kg^{-1} and 9.14 ± 3.45 mg g^{-1}), followed by RFs (14.87 ± 2.06 m^2 kg^{-1} and 7.56 ± 2.03 mg g^{-1}) and CPs

($11.99 \pm 1.45\,m^2\,kg^{-1}$ and $4.99 \pm 0.66\,mg\,g^{-1}$). Both traits showed statistically significant differences across land covers (ANOVA p value < 0.002 for SLA_{cwm}, p value < 0.018 for Chl_{cwm}). In contrast, $LDMC_{cwm}$ did not differ substantially among land-cover classes (p value $= 0.51$), with CPs having the highest value ($407.64 \pm 21.68\,mg\,g^{-1}$), followed by EFs ($398.43 \pm 72.24\,mg\,g^{-1}$) and RFs ($370.13 \pm 94.97\,mg\,g^{-1}$). See Table S8 for data sources and shared percentages of species trait values used to compute SLA_{cwm}, Chl_{cwm}, and $LDMC_{cwm}$.

3.4 Stand structure attributes

3.4.1 DBH and tree height

Land-cover conversion reduces both the mean and variability for tree diameter and height, indicating a loss of structural complexity in human-disturbed ecosystems. Structural measurements of 292 woody trees across three land-cover classes showed that EFs had the highest structural complexity, with the highest mean and variability in DBH (18.0 ± 20.1 cm) and tree height (17.0 ± 13.3 m), including the largest individuals (DBH = 102.3 cm, $H = 52.0$ m; Fig. S9). However, RFs and CPs had substantially lower means and variability in these variables, suggesting reduced structural complexity after forest conversion. While both RFs and CPs had similar heights (RF: 7.4 ± 3.8 m; CP: 6.3 ± 1.0 m), CPs had a significantly greater DBH (CP: 13.0 ± 3.9 cm; RF: 5.8 ± 4.3 cm). The results of the ANOVA and Tukey HSD tests confirmed significant differences in DBH and height among land covers (p value < 0.001), except for EFs and CPs for DBH and RFs and CPs for height (Table 3).

3.4.2 Aboveground and deadwood biomass

Land-cover conversion from EFs to RFs and CPs resulted in a substantial decline in both aboveground and deadwood biomass. The mean AGB_f estimated using the generic allometric function dropped sharply from $239 \pm 92\,Mg\,ha^{-1}$ in EFs to $42 \pm 10\,Mg\,ha^{-1}$ in RFs and $71 \pm 22\,Mg\,ha^{-1}$ in CPs. Similarly, the mean total DWB declined from $27.5 \pm 12.4\,Mg\,ha^{-1}$ in EFs, $4.8 \pm 7.0\,Mg\,ha^{-1}$ in RFs, and $0.4 \pm 0.2\,Mg\,ha^{-1}$ in CPs. See Table A1 for the contribution of lying and standing DWB to total DWB.

3.4.3 Stem density and basal area

Changes in land cover strongly influenced stem density, basal area, and the distribution of aboveground biomass across DBH classes (Fig. 3). RFs exhibited twice the stem density (DBH > 5 cm) per hectare compared to EFs and CPs, driven largely by a high proportion of smaller trees in the 5–15 cm DBH class. Despite having a lower mean DBH, RFs had a higher basal area ($17.0 \pm 5.4\,m^2\,ha^{-1}$) than CPs ($11.6 \pm 3.5\,m^2\,ha^{-1}$). Interestingly, in EFs, only 5 % of the stems with a DBH > 30 cm contributed to approximately 65 % of the total AGB_f. In contrast, the main DBH class contributing to the AGB_f in RFs and CPs was 5–15 cm, accounting for 57 % and 76 % of the total AGB_f in RFs and in CPs, respectively. Refer to Table S9 in the Supplement for shared stem density percentages per hectare across DBH classes and Table S10 for shared percentages of AGB_f categorized by DBH class.

3.4.4 LAI and fPAR

The mean total leaf area index values were $6.16 \pm 0.67\,m^2\,m^{-2}$ for EFs, $5.57 \pm 0.76\,m^2\,m^{-2}$ for RFs, and $3.07 \pm 0.61\,m^2\,m^{-2}$ for CPs. The mean canopy LAI values were $4.62 \pm 0.5\,m^2\,m^{-2}$ for EFs, $4.66 \pm 0.70\,m^2\,m^{-2}$ for RFs, and $2.52 \pm 0.42\,m^2\,m^{-2}$ for CPs. The ANOVA analysis revealed a significant difference in mean LAI_T and mean LAI_C among the three land-cover classes, while the Tukey HSD test did not find a significant difference in mean LAI_T and mean LAI_C between EFs and RFs (Table 3). The phenology of both LAI_T and LAI_C revealed a similar pattern in EFs and RFs, with peak and base values in June and March, respectively (Fig. 4a–b, Table S11). The LAI_T and LAI_C patterns for CPs resembled those of EFs and RFs but also had a strong decrease in April. Furthermore, the understorey LAI (LAI_U; the difference between LAI_T and LAI_C) for the various land-cover classes indicates that the ground vegetation greatly contributes to LAI_T for EFs and RFs, while the contribution was minor for CPs (Fig. 4c). In particular, the LAI_U mean values within 1 year were approximately $1.54 \pm 0.57\,m^2\,m^{-2}$ for EFs (25 %), $0.91 \pm 0.36\,m^2\,m^{-2}$ for RFs (16 %), and $0.55 \pm 0.39\,m^2\,m^{-2}$ for CPs (18 %). A general trend of a high contribution of LAI_U to LAI_T in June and a low contribution in April was apparent for all land-cover classes.

The observed mean annual fPAR for EFs, RFs, and CPs was high: 0.97 ± 0.01, 0.96 ± 0.01, and 0.76 ± 0.06, respectively (Table 3). The values of EFs and RFs exhibited minimal fluctuations throughout the year, whereas the fPAR of CPs ranged between 0.55 and 0.93 (Fig. 5). Like LAI, the annual mean fPAR among EFs, RFs, and CPs was statistically significantly different according to both the ANOVA and Tukey HSD tests.

3.5 Estimated aboveground biomass based on DBH–H relationship

3.5.1 DBH–H relationship

Land-cover change weakens tree allometry, reducing the consistency of DBH–H relationships in human-impact forest and agricultural ecosystems. Strong positive relationships between DBH and H were observed in both EFs and RFs. For EFs, 92 % of the variation in H can be explained by the variation in DBH, whereas, for RFs and CPs, it was 78 % and 51 %, respectively (Fig. 6, Table S12). The power-law

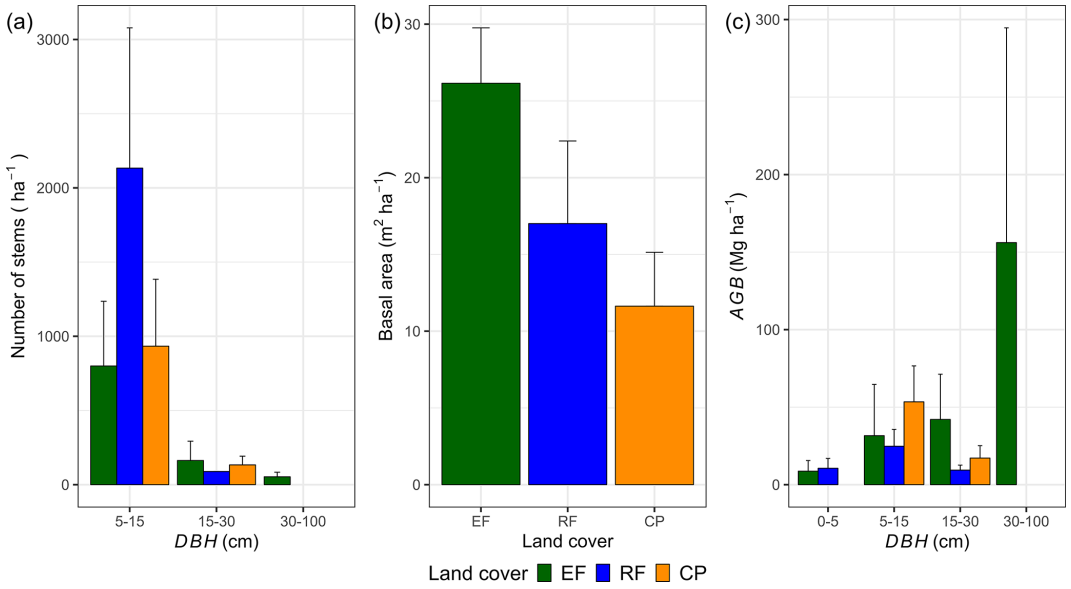

Figure 3. Estimations per land-cover class of a mean number of stems per hectare **(a)**, basal area (BA; $m^2\ ha^{-1}$) **(b)**, and mean aboveground biomass separated by the different classes of diameter at breast height (DBH) **(c)**. In panel **(c)**, the contribution of different DBH classes to the mean aboveground biomass estimated by the AGB_f method was used in this calculation. The error bars in the figure represent 1 standard deviation.

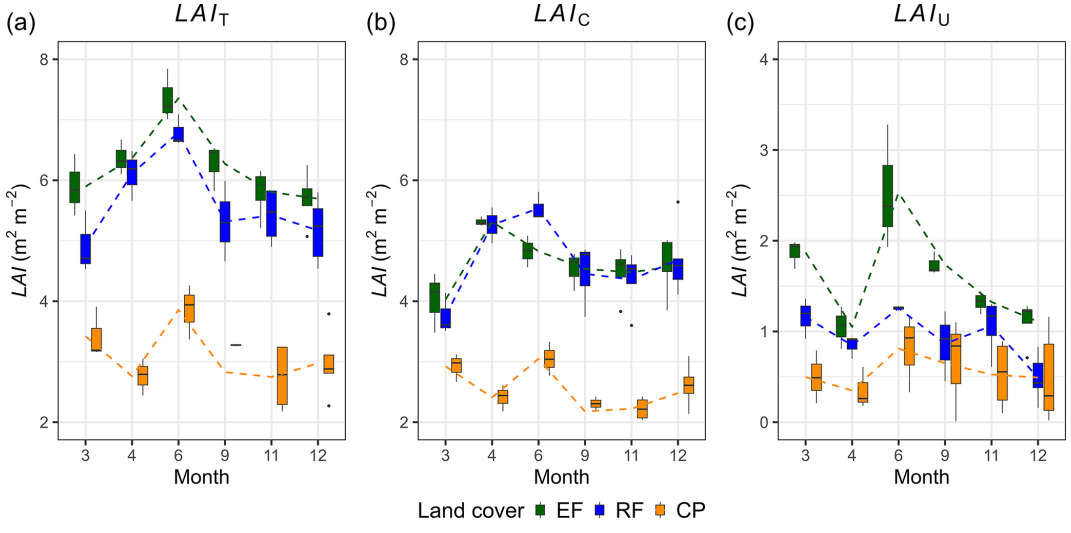

Figure 4. Total leaf area index (LAI_T; $m^2\ m^{-2}$), canopy leaf area index (LAI_C; $m^2\ m^{-2}$), and understorey leaf area index (LAI_U; $m^2\ m^{-2}$) and their variations across different months within 1 year for evergreen forests (EFs), regrowth forests (RFs), and cashew plantations (CPs). The lines on the graph represent the connection between the mean LAI values from 1 month to another.

relationships between DBH and H further indicated that the K_1 and K_2 values for EFs and RFs were similar, whereas the values for CPs were much lower. For a plot-level analysis of relationships between ln(DBH) and ln(H), see Fig. S10 and Table S13.

3.5.2 Comparison of AGB estimation methods

Our results indicate that locally calibrated DBH–H relationships and species-specific wood density substantially affected aboveground biomass estimates compared to generalized models (Fig. 7). The AGB_{wd} method consistently produced higher values than AGB_f across all land-cover classes, reflecting the influence of wood density and the dominance of high-density tree species at our study site. In EFs and

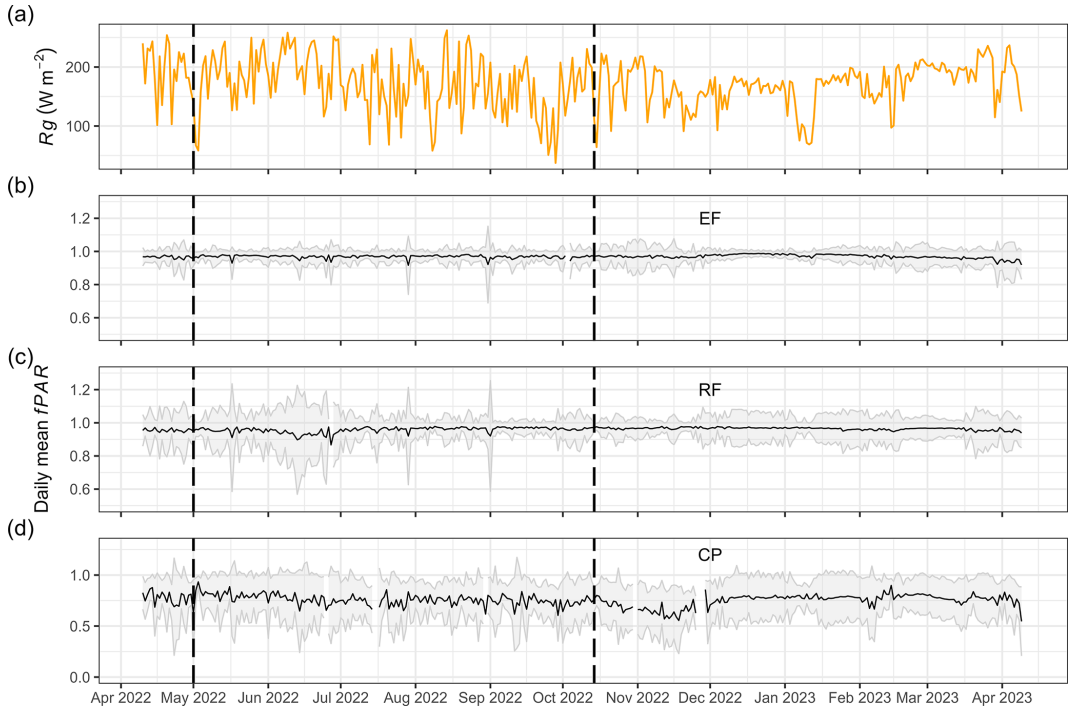

Figure 5. Daily mean global radiation (Rg; W m^{-2}) **(a)** and daily mean fPAR for evergreen forests (EFs) **(b)**, regrowth forests (RFs) **(c)**, and cashew plantations (CPs) **(d)** from 11 April 2022 to 9 April 2023 at Kulen. The shaded area represents 1 standard deviation from the mean, computed using the 10 PAR sensors installed in each land-cover class.

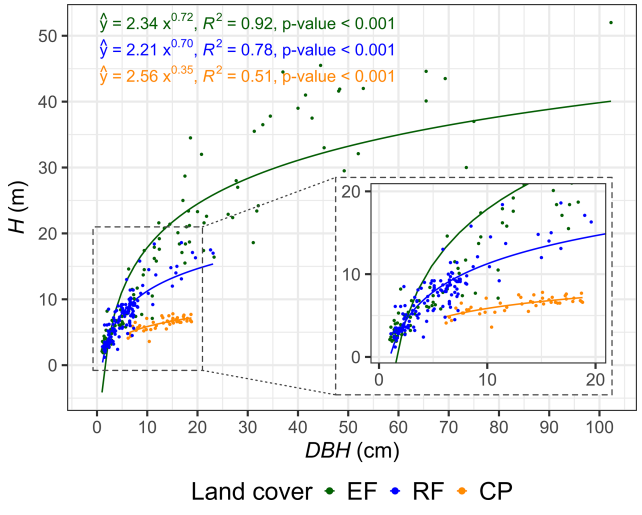

Figure 6. Relationship between diameter at breast height (DBH) (cm) and tree height (H) (m) for evergreen forests (EFs), regrowth forests (RFs), and cashew plantations (CPs) in Kulen. The figure shows the derived power-law intercept (K_1) and slope (K_2) values for EFs, RFs, and CPs.

RFs, where DBH–H relationships were strong, AGB_h estimates were markedly higher than AGB_f (EFs: 312 ± 184 vs. 239 ± 92 Mg ha^{-1}; RF: 54 ± 14 vs. 42 ± 10 Mg ha^{-1}), consistent with plot-level regression results (Fig. S10, Table S13). In contrast, in CPs, AGB_h yielded much lower values than AGB_f (17 ± 5 vs. 71 ± 22 Mg ha^{-1}), highlighting the limited reliability of this method under weak DBH–H relationship conditions. The differences between AGB_h and AGB_f estimates across land covers are illustrated in 1 : 1 comparison plots and plot-level summaries (Figs. S11–S13).

3.6 AGB_h relationships with LAI_T, SLA_{cwm}, and S_R

We observed positive relationships between aboveground biomass and three pivotal ecosystem characteristics: LAI_T, S_R, and SLA_{cwm} determining 76 %, 72 %, and 68 % of the variability in AGB, respectively (see Fig. 8 and Table S14 for statistical regression tables). LAI_T exhibited strong positive correlations with SLA_{cwm}, S_R, and AGB, with the Pearson correlation coefficient in the range of 0.67–0.85. SLA_{cwm} had a positive correlation with S_R and AGB. Furthermore, additional insights regarding the Pearson correlation matrix depicting relationships among various ecosystem characteristics are presented in Fig. S14.

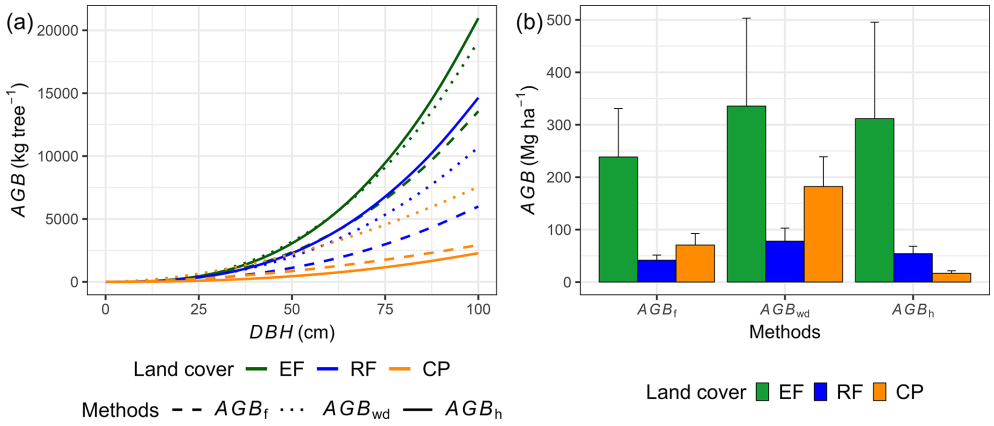

Figure 7. Power-law relationships between aboveground biomass (AGB) of AGB_f, AGB_h, and AGB_{wd} and diameter at breast height (DBH) for each land-cover class **(a)**, along with the corresponding results of AGB estimation **(b)**. AGB_f represents aboveground biomass estimated by adopted functions, AGB_{wd} represents aboveground biomass estimated by adopted functions utilizing species-specific wood density, and AGB_h represents aboveground biomass estimated by the DBH and tree height (H) relationship, in conjunction with species-specific wood density, for the study site. The error bar in panel **(b)** represents 1 standard deviation.

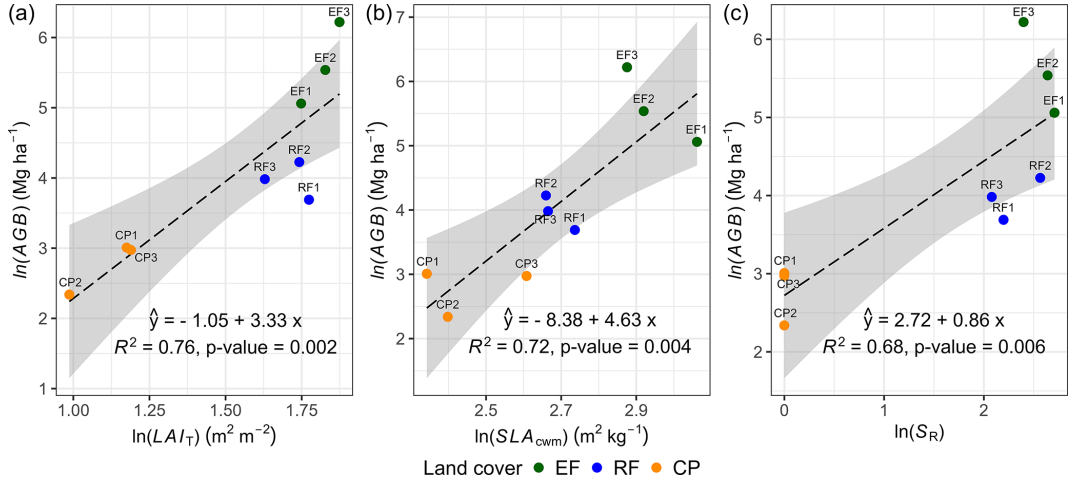

Figure 8. Ordinary least-squares regression showing the effect of mean total LAI (LAI_T; m^2 m^{-2}), mean SLA_{cwm} (m^2 kg^{-1}), and species richness (S_R; count per plot) on AGB. Mean LAI_T is a mean ground LAI measurement; S_R is a woody species count excluding seedlings in a plot; and AGB is AGB_h, whose estimation was based on the DBH–H relationship.

4 Discussion

4.1 Soil conditions

The observations of soil temperature, soil water content, and soil electrical conductivity all support our hypothesis that land-cover conversion changes soil conditions in these tropical forest ecosystems. The difference in soil temperature between the forested land-cover classes (EFs and RFs) and the cashew plantations (Table 3) aligns with prior studies by van Haren et al. (2013) and Geng et al. (2022) and can be explained by the substantial difference in interception of incoming radiation between these ecosystems (Fig. 4). The multi-layered canopies and the dense layer of deadwood and litterfall, effectively prevent direct sunlight from reaching the ground. This natural shield reduces the impact of solar irradiance, thereby maintaining cooler soil surface temperatures (Senior et al., 2018). Conversely, CPs have a simpler canopy structure, predominantly featuring a single layer of cashew trees of similar age. The understorey in these areas is sparser, and the reduction in deadwood, due to management, facilitates greater penetration of solar irradiance and elevates soil temperatures.

Our observed annual mean soil water content across the three land-cover classes (0.14–0.23 m^3 m^{-3}) is consistent with earlier findings (Rodell et al., 2004; Wang et al., 2012; Horel et al., 2022). Variations in SWC among these classes may stem from differences in their stand structural complexity (vegetation cover and root system) and soil properties

(organic matter content and texture) (Pickering et al., 2021; Tang et al., 2021). The higher SWC in evergreen forests compared to regrowth forests is attributed to their dense and multi-layered vegetation cover, which reduces penetration of solar irradiance and temperature at the forest floor, thereby reducing evaporation and maintaining topsoil moisture (Fig. 4). In addition, the complex root systems of primary forests enhance water retention by creating channels and pores in the soil, while organic matter from deadwood and litterfall further enhances soil water retention, particularly during arid conditions (Luo et al., 2023). Another explanation could be the soil texture, as our field investigation observed that cashew plantations are all on sandier soils with lower water-holding capacity, leading to decreased SWC (Ibrahim and Alghamdi, 2021). Nevertheless, further examination of soil samples is necessary to accurately measure the specific soil properties in each land-cover class.

The analysis of soil electrical conductivity categorized the soils as non-saline across the land-cover classes. Evergreen forests had higher ECs than cashew and regrowth forests, potentially indicating larger nutrient availability (Omuto et al., 2020). This higher nutrient availability in evergreen forests may be linked to greater organic matter decomposition, greater species richness, higher soil moisture content, and no history of being clear-cut, which could lead to nutrient losses via run-off during the phase without vegetation (Austin et al., 2004; Vestin et al., 2020; Guo et al., 2023b).

4.2 Species diversity

Species richness and Shannon–Wiener index clearly declined from evergreen forests to regrowth forests and were lowest in cashew plantations, supporting our hypothesis that land-cover conversion reduces species diversity. While EFs and RFs showed similar mean values to other evergreen forests in the mainland of Southeast Asia and India (Zin and Mitlöhner, 2020; Theilade et al., 2022; Tynsong et al., 2022), S_R was lower compared to the most diverse rainforests in South America and equatorial Southeast Asia, where >250 species ha^{-1} have often been reported (Suratman, 2012; ter Steege et al., 2023), and S_H was lower than for some moist evergreen and humid lowland forests in the region (Mohd Nazip, 2012; Zin and Mitlöhner, 2020). These tropical rainforests may have more species because of their larger forest patch sizes and higher rainfall, compared to the relatively isolated monsoon forest at the top of Kulen, surrounded by agricultural areas (Galanes and Thomlinson, 2009). The relatively low S_H may also be explained by the high proportion of the top five dominant species in each land cover, accounting for over 50 % of total stems in their communities. Another possible reason could be the limited number of sample plots, which may not fully capture the overall species composition and distribution in these forests. Tropical tree species composition is markedly influenced by biogeography and disturbance history, showing significant local variations even over short distances (Whitmore, 1998; Van and Cochard, 2017). This emphasizes the necessity for comprehensive field data sampling to accurately assess the species richness and evenness of these highly diverse plant communities. The comparison between S_R and S_H of EFs and RFs in previous studies is presented in Tables S15–S16.

4.3 Leaf functional traits

Specific leaf area, leaf dry matter content, and chlorophyll content are all key leaf traits in the leaf economic spectrum and carry diverse implications for understanding carbon sequestration, resource availability, successional stages, and environmental responses (Wright et al., 2004; Gao et al., 2022). Our results support the hypothesis that changing from pristine evergreen forests to regrowth forests and cashew plantations leads to a substantial decline in key leaf functional traits, particularly specific leaf area and chlorophyll content, indicating reduced ecosystem productivity and resource-use efficiency.

Our observations emphasize the significant consequences of transitioning from EFs to RFs or CPs, resulting in a substantial reduction in actual values and diversity in SLA_{cwm}, reflecting a reduction in both ecosystem productivity and resilience to disturbances (Liu et al., 2023). The higher SLA_{cwm} in EFs suggests higher photosynthetic capacity, especially in shaded environments, due to its dense canopy cover and abundant resource availability (water and nutrients) for plant growth (Green et al., 2020). High SLA_{cwm} values also link to faster turnover and promote nutrient cycles, carbon sequestration, and nutrient use efficiency in forest ecosystems (Guerrieri et al., 2021). The lower SLA_{cwm} values of RFs and CPs may be attributed to limited water and nutrient availability in the soil because of high competition in those ecosystems. The notable reduction in SLA_{cwm} caused by the shift from EFs to RFs or CPs underlines the profound impact land-cover change has on ecosystem productivity, resilience, and overall functioning. Our SLA_{cwm} of EFs exceeded the mean values of tropical forests in Bolivia, Brazil, Costa Rica, and China (Finegan et al., 2015; Wang et al., 2016). The SLA_{cwm} of RFs was somewhat higher than the mean of neotropical regrowth forests but still within the range (Poorter, 2021). SLA_{cwm} in CPs was greater than the range value in Parakou, Benin, but fell within the range reported for 15 cashew varieties in Karnataka, India (Akossou et al., 2016; Mog and Nayak, 2018).

Chlorophyll is essential for photosynthesis and serves as a crucial indicator of a plant's photosynthetic capacity, profoundly influencing overall growth (Stirbet et al., 2020). The elevated Chl_{cwm} seen in EFs can be attributed to the well-developed and dense canopy structure, which creates a light-shaded environment. This prompts plants to invest more in chlorophyll production, enhancing light harvesting efficiency (Niinemets, 2010). Meanwhile, RFs, experiencing intense competition for light in early successional stages, may ex-

hibit lower chlorophyll levels as resources prioritize vertical growth over chlorophyll production (Laurans et al., 2014). Our CPs had lower Chl_{cwm} than EFs and RFs due to less light competition and higher temperatures, which could lead to photoinhibition and lowered leaf chlorophyll content (Rosa et al., 2020). Our Chl_{cwm} of EFs and RFs falls within the range but surpasses the mean Chl_{cwm} observed in Chinese forest ecosystems (Li et al., 2018).

Leaf dry matter content is a measure of construction cost per fresh weight mass unit, and it serves as a metric for a plant's resource use strategy and resilience to environmental stresses (Guo et al., 2023a). The higher $LDMC_{cwm}$ in EFs compared to that of RFs indicates a conservative resource usage, longer leaf lifespan, and increased carbon sequestration, implying higher ecosystem stability and function for EFs (Rawat et al., 2021). Conversely, the highest $LDMC_{cwm}$ in CPs is attributed to cashew monoculture and the species' high resilience to environmental stress, especially in nutrient-poor soils and water-stressed conditions (Bezerra et al., 2007). This study emphasizes the increased stress tolerance, conservative resource utilization, and greater carbon sequestration of EFs compared to RFs, while also emphasizing cashew as a highly proficient species in environmental stress tolerance.

4.4 Stand structure attributes

4.4.1 DBH and tree height

Our findings confirm significant differences in mean DBH and tree height resulting from the conversion of pristine evergreen forests to young regrowth forests and cashew plantations following human disturbance. The observed reduction in large-diameter and tall trees in regrowth forests and cashew plantations compared to the evergreen forests (Fig. 3) provides clear evidence of structural degradation, which negatively affects crucial key ecosystem functions such as carbon storage, nutrient cycling, and biodiversity (Díaz et al., 2007; Lutz et al., 2018; Thiel et al., 2021). Observed species in our evergreen forests, such as *Dipterocarpus costatus*, *Sandoricum indicum*, *Mesua ferrea*, *Nageia wallichiana*, and *Litchi chinensis*, reach heights of 40–52 m, similar to those found in Cambodia's central evergreen forests (Theilade et al., 2022). Our mean DBH of evergreen forests is comparable to mature tropical forests in Vietnam and falls within the pantropical range, while regrowth forests have a slightly higher mean DBH than tropical secondary forests in Sarawak, Malaysia (Brown, 1997; Kenzo et al., 2009; Yen and Cochard, 2017). In contrast, cashew plantations show a significantly lower mean DBH compared to older counterparts in Kampong Cham, Cambodia (Avtar et al., 2013).

4.4.2 Aboveground and deadwood biomass

Our results support that land-cover conversion reduces in aboveground and deadwood biomass in regrowth forests and cashew plantations compared to in evergreen forests. The substantial decline in aboveground biomass following conversion from EFs to RFs or CPs is primarily driven by historical human disturbance, particularly clear-cutting and the removal of large trees, as evidenced by reduced DBH and tree height in this study. Similarly, DWB decreased as EFs were replaced by RFs and CPs, reflecting the impacts of land-cover change on forest biodiversity and ecosystem health. DWB is a key indicator of biodiversity and ecosystem health, supporting various species and ecosystem processes such as carbon and nitrogen cycling, soil fertility enhancement, pollination, and erosion control (Parisi et al., 2018; Santopuoli et al., 2021; Tláskal et al., 2021). Variations in total DWB values could result from the degree of disturbances within the studied forests (Baker et al., 2007). The higher DWB in EFs is due to their old stand age, long-term accumulation of DWB, and absence of slash-and-burn practice as observed in RFs and CPs (van Galen et al., 2019). In CPs, some farmers periodically cut and burn dead branches of cashew trees to promote growth. Consistent with these trends, DWB in our EFs and RFs was comparable to previous studies in Cambodia and Malaysia (Saner et al., 2012; Kiyono et al., 2018), whereas our CPs have less DWB than plantations in Cameroon (Victor et al., 2021).

4.4.3 Stem density and basal area

The land-cover change alters stem density across EFs, RFs, and CPs. Our mean stem density per hectare of evergreen forests is consistent with previous studies in Cambodia, Vietnam, and Borneo, while regrowth forests show lower densities compared to those in the Yucatan Peninsula, Mexico (Slik et al., 2010; Con et al., 2013; Román-Dañobeytia et al., 2014; Chheng et al., 2016; Theilade et al., 2022). Additionally, our stem density in cashew plantations is similar to that of Isuochi, Nigeria, but significantly greater than that of Casamance, Senegal, due to their differences in planting distance and management practices (Nzegbule et al., 2013; Ndiaye et al., 2020). The variation in stem density between evergreen forests and regrowth forests reflects distinctive stages of succession. In the early succession stage following clearance, open niches and resource abundance create a favourable environment for fast-growing and highly reproductive early-succession species, resulting in higher stem density and heightened interspecies competition (Zhang et al., 2020). As the forest matures, stem density naturally decreases as larger trees occupy more space and take more of the light, water, and nutrient resources. This competition ultimately leads to the mortality of smaller trees, aligning with the power-law relationship between stem density and biomass commonly observed in mature forests (Mrad et al.,

2020). This natural process also alters species composition, stand structure, habitat heterogeneity, and biomass of forests (Forrester et al., 2021). In cashew plantations, stem density is controlled by humans to enhance cashew yield. This alteration in stand structure complexity influences interspecies competition. These modifications also affect stand structure and interspecies competition, ultimately influencing the biodiversity and functioning of the ecosystem.

Basal area also decreases significantly when EFs are replaced with RFs or CPs, impacting biomass, productivity, stand structure, and structural complexity (Gea-Izquierdo and Sánchez-González, 2022). RFs have a lower BA than EFs, indicating early succession and disturbance (Ziegler, 2000). Despite the fact that tropical forests possess natural regenerative capabilities, RFs may require several decades to achieve BA levels comparable to EFs, highlighting the critical importance of conserving EFs to maintain their ecological integrity and ecosystem services. In addition, the basal area of evergreen forests in our study aligns with those in northeastern Cambodia and Pahang National Park, Malaysia, but falls below values reported for Laos, Cambodia's central plains, and Vietnam's lowlands (Rundel, 1999; Sovu et al., 2009; Suratman, 2012; Chheng et al., 2016; Theilade et al., 2022). Our regrowth forest's BA exceeds that of regrowth forest in Laos, while the BA of our cashew plantations surpasses that of plantations in Tanzania (Sovu et al., 2009; Malimbwi et al., 2016).

4.4.4 LAI and fPAR

LAI and fPAR differed markedly among the three land-cover classes, reflecting structural changes in canopy structure associated with land-cover conversion consistent with our hypothesis. In our study, the canopy leaf area index in evergreen forests surpasses that of dry evergreen forests in Kampong Thom, Cambodia, while regrowth forests lie between those of 18–35-year tropical secondary forests in Costa Rica; however, cashew plantations exceed reported values in India (Ito et al., 2007; Clark et al., 2021; Kumaresh et al., 2023). The LAI_C difference between the forests (EFs and RFs) and CPs was significant due to CP management practices, resulting in a thin canopy with low LAI_C. In contrast, natural forests with their densely developed canopy have a high LAI_C. Additionally, LAI_C phenology followed the rainy and dry seasons, with peak values during the rainy season and low values during the dry season (Ito et al., 2007). During the dry season, reduced rainfall leads to less water availability for plant growth, causing plants to adapt to water stress by shedding their leaves, resulting in low LAI_C in the ecosystem (Maréchaux et al., 2018). The comparison between LAI_C and LAI_T of EFs and RFs in previous studies is presented in Table S17.

Our mean fraction of photosynthetically active radiation for EFs and RFs marginally exceeded the global range for broadleaf forests and the monthly range observed in the Amazon tropical forest in Santarém, Brazil (Senna et al., 2005; Pastorello et al., 2020). The fPAR for CPs, on the other hand, is within the range values reported for broadleaf crops (Xiao et al., 2015). Despite annual variations in LAI_C (24 % for EFs, 32 % for RFs, 29 % for CPs) and incoming solar irradiance, fPAR remained remarkably stable throughout the year in the forest ecosystems (EFs and RFs; Fig. 5). This stability can be attributed to the exponential relationship between fPAR and LAI, which typically saturates at LAI above 3 (Dawson et al., 2003). Our recorded lowest LAI for EFs and RFs was 3.48, likely contributing to this saturation and explaining the lack of phenology displayed in fPAR. The exclusion of reflected PAR above the canopy in the fPAR estimation may also contribute to the stability; however, previous studies have shown that the difference between intercepted (what we measured) and absorbed PAR (including the reflected component) is minimal (Olofsson and Eklundh, 2007).

Despite an increased stem density in RFs compared to EFs and a similar canopy LAI and fPAR, our observations of significant differences in mean DBH, tree height, and basal area; the reduction in aboveground and deadwood biomass; the altered stem density; and the reduction in contribution of understorey LAI to total LAI support our hypothesis that the land-cover change causes a decreased complexity in stand structure.

4.5 Estimated aboveground biomass based on DBH–*H* relationship

4.5.1 DBH–*H* relationship

Variation in the strength of DBH–*H* relationships reflects different disturbance histories in EFs and RFs and the influence of management practices in CPs. The DBH–*H* relationship is crucial for understanding variations in tree growth rates, successional stage, aboveground biomass, and forest health (Kramer et al., 2023). Finding a strong positive DBH–*H* relationship may indicate disturbances within the ecosystem; by initiating gaps in the canopy, such disturbances provide opportunities for fast-growing species to establish and utilize increased light availability and resources within the ecosystem (Senf et al., 2020). Hence, the observed relationships between EFs and RFs suggest a composition of fast-growing species and indicate that EFs may have experienced past disturbances. Indeed, a windthrow in EF1 is reflected in its lowest LAI_C among EF plots and a smaller mean DBH (Table 1, Fig. S9a).

The lower DBH–*H* relationship in cashew plantations results from the growth strategy of the single species and management practices. In monocultures with uniformly aged cashew plants, competition for light and resources is comparable, resulting in a consistent resource distribution. Cashew's natural growth characteristics, with the species reaching up to 15 m in height and a DBH of 100 cm under

favourable conditions (Avtar et al., 2014), indicate a preference for investing resources in branches and stems over height, especially in low-light competition environments. However, our observations indicate significant variation in the DBH–H relationship among CP plots (low R^2 value in Figs. 6, S10g–i), which may have been influenced by their different management practices, such as spacing, pruning, and thinning. These practices impact the DBH–H relationship by minimizing light competition, resulting in a higher DBH–H ratio which also affects the relationship (Deng et al., 2019; Bhandari et al., 2021).

4.5.2 Comparison of AGB estimation methods

Our results suggest that locally calibrated DBH–H relationships and wood density substantially affect AGB estimates compared to generalized models, supporting the feasibility of site-specific calibration, particularly for natural forest ecosystems. Recent studies have emphasized the significant uncertainty in estimating plot-level aboveground biomass when directly applying a generic AGB allometric equation (AGB_f) due to variations in species composition and stand structure between the study site and the equation's origin (Feldpausch et al., 2011; Burt et al., 2020). To address this challenge, our study proposes an allometric approach (AGB_h) using local species-specific wood density and the DBH–H relationship at the study site. This approach captures the unique characteristics of the site's species composition and stand structure (Ketterings et al., 2001; Nyirambangutse et al., 2017). Our locally adopted AGB_h method produced estimates $\sim 30\,\%$ higher than the generic AGB_f for both EFs and RFs (Table 3, Fig. 7b). This is likely due to the combined effects of higher mean wood density and a stronger DBH relationship, resulting in a more pronounced exponential growth response in AGB (Fig. 7a). Still, these $\sim 30\,\%$ higher values align with the range reported in previous studies (Tables A2–A3). In contrast, in the CP case, our AGB_h method produced estimates less than one-quarter of the generic AGB_f method. The reason is that the AGB_h method is less reliable when a weak DBH–H relationship is detected because it fails to accurately capture the overall tree size and volume. This is also reflected in the substantially larger uncertainty as indicated by the standardized errors of the parameters within the DBH–H relationship (Tables A4, S12). The substantial difference between AGB_{wd} and AGB_f is primarily due to the wood density values used, $0.45\,g\,cm^{-3}$ from Zanne et al. (2009) in this study versus $0.18\,g\,cm^{-3}$ in the original AGB_f equation (Mlagalila, 2016), likely reflecting variation in cashew wood properties or wood density measurement protocols among the two studies. Despite clear differences in Fig. 7b, formal statistical comparisons were not conducted due to the limited number of plots per class ($n = 3$), which restricts statistical power. However, to fully validate the AGB allometric equations, destructive field-observed data would be necessary. Therefore, future research should include direct field measurements of AGB to more accurately validate the methods for these land-cover classes.

4.6 AGB_h relationships with LAI_T, SLA_{cwm}, and S_R

Exploring the relationship between aboveground biomass and key ecosystem characteristics, such as leaf area index, specific leaf area, and species richness, is vital for comprehending the complexity of ecosystem dynamics and informing ecosystem modelling. We observed a strong positive relationship between LAI_T and AGB_h, supporting prior findings (He et al., 2021; Zhao et al., 2021). Higher LAI_T enhances light interception and results in higher biomass. Elevated AGB_h levels stimulate LAI_T expansion by providing resources for robust leaf growth, leading to a denser canopy and greater leaf coverage. Similarly, our findings support a positive relationship between SLA_{cwm} and AGB_h (Finegan et al., 2015; Ali et al., 2017; Gao et al., 2021). Higher SLA_{cwm} values indicate a plant community with improved photosynthetic capacity, nutrient uptake, and leaf turnover, which is essential for nutrient cycling (Reich et al., 1991). An increase in AGB_h has a reinforced effect on SLA_{cwm} values, suggesting enrichment of the soil nutrient pool and providing structural support for plant growth. This influences light availability and competition dynamics, affecting leaf morphology and SLA_{cwm}. Furthermore, the positive relationship between AGB_h and S_R is widely observed and explained by the niche complementarity hypothesis (Waide et al., 1999; Jactel et al., 2018; Steur et al., 2022). This concept suggests that an ecosystem with high species diversity has a greater variation in functional traits and resource-use strategies, lowering competition for scarce resources and thus promoting productivity (Tilman et al., 1997). In return, an increase in AGB_h fosters the coexistence of diverse species by providing more available resources and habitat complexity in an ecosystem, thereby increasing species richness.

5 Conclusions

In response to growing concerns over the ecological impacts of forest conversion in tropical Southeast Asia, we investigated how land-cover change from pristine evergreen forests to regrowth forests and cashew plantations alters stand structure, species diversity, leaf functional traits, and soil conditions, and we evaluated the feasibility of locally calibrated DBH–H allometries for improving aboveground biomass estimation. Our findings confirm our hypotheses that land-cover change reduces stand structural complexity, species composition, and leaf functional traits and causes a substantial change in soil conditions. We further demonstrate the utility of our novel dataset for improving aboveground biomass estimation through the application of an allometric function based on locally specific WD and the DBH–H rela-

tionship. This approach has great potential for improving carbon stock estimations and promoting informed forest management practices. However, as we lack direct destructive samples of aboveground biomass, we can neither reject nor support our second hypothesis that locally calibrated DBH–H relationships would substantially improve aboveground biomass estimates compared to generalized models. Moreover, our analysis of relationships between leaf area index, specific leaf area, species richness, and aboveground biomass underlines the profound impact of land-cover change on ecosystem productivity and functioning in these tropical forest regions. To strengthen and extend these findings, future studies should incorporate destructive sampling to validate our locally calibrated aboveground biomass allometric equations based on DBH–H relationships and WD. Expanding field data collection by increasing the number and spatial distribution of plots across a broader range of land-use classes in tropical Southeast Asia and promoting open data sharing will be critical for improving our understanding of ecosystem responses to forest conversion and supporting sustainable forest management under global change in the region.

Appendix A

Table A1. Estimated lying deadwood biomass (Mg ha^{-1}), standing deadwood biomass (Mg ha^{-1}), and total deadwood biomass (Mg ha^{-1}) by different land-cover classes in Kulen. Mean ± SD is the mean plus or minus 1 standard deviation.

Land cover	Lying deadwood biomass (Mg ha^{-1})		Standing deadwood biomass (Mg ha^{-1})		Total deadwood biomass (Mg ha^{-1})	
	Mean ± SD	Range	Mean ± SD	Range	Mean ± SD	Range
EF ($n = 3$)	17.74 ± 19.93	1.64–40.03	9.74 ± 8.49	0–15.56	27.48 ± 12.37	15.31–40.03
RF ($n = 3$)	3.65 ± 5.32	0.48–9.79	1.16 ± 1.66	0–3.06	4.81 ± 6.97	0.48–12.85
CP ($n = 3$)	0.40 ± 0.19	0.28–0.62	0	0	0.40 ± 0.19	0.28–0.62

Table A2. Comparing estimated aboveground biomass (AGB; Mg ha^{-1}) in evergreen forests (EFs) using adopted allometric equations (AGB_f), the diameter at breast height (DBH) and tree height (H) power-law relationship (AGB_h), and previous AGB reported in previous studies. Mean ± SD is the mean plus or minus 1 standard deviation.

No.	Region	Vegetation type	AGB (Mg ha^{-1})		References
			Mean ± SD	Range	
1	Kulen, Cambodia	Tropical evergreen forest	311.66 ± 183.88	147.53–510.57	AGB_h in this study
2	Kulen, Cambodia	Tropical evergreen forest	238.53 ± 92.41	161.83–341.13	AGB_f in this study
3	Global	Tropical forest	379.02 ± 187.40	230.58–589.58	Chave et al. (2014)
4	Gia Lai, Vietnam	Tropical evergreen forest	273.24 ± 112.22	189.53–400.76	Nam et al. (2016)
5	Mondulkiri, Cambodia	Tropical moist evergreen forest	333.00 ± 137.00	78.00–837.00	Sola et al. (2014)
6	Borneo (Brunei, Malaysia, Indonesia)	Tropical lowland evergreen forest	458.16 ± 123.62	196.30–778.50	Slik et al. (2010)
7	Thanh Hoa, Vietnam	Tropical evergreen broadleaf forest	251.81 ± 125.43	40.88–543.88	Nguyen and Kappas (2020)
8	Africa	Tropical evergreen forest	429.00	114.00–749.00	Lewis et al. (2013)
9	Cambodia	Evergreen forest	243.00 ± 128.00	11.00–837.00	Sola et al. (2014)
10	Kampong Thom, Cambodia	Evergreen forest	294.00 ± 65.00	176.00–398.00	Ota et al. (2015)
11	Vietnam	Tropical evergreen broadleaf forests in various ecoregions	230.10 ± 8.60	199.00–320.20	Van Do et al. (2019)

Table A3. Comparing estimated aboveground biomass (AGB; Mg ha^{-1}) in regrowth forests (RFs) using adopted allometric equations (AGB_f), the diameter at breast height (DBH) and tree height (H) power-law relationship (AGB_h), and previous AGB reported in previous studies. Mean ± SD is the mean plus or minus 1 standard deviation.

No.	Region	Vegetation type	AGB (Mg ha^{-1})		References
			Mean ± SD	Range	
1	Kulen, Cambodia	Natural regrowth evergreen forest	54.19 ± 14.09	38.26–65.04	AGB_h in this study
2	Kulen, Cambodia	Natural regrowth evergreen forest	41.66 ± 9.82	31.60–51.21	AGB_f in this study
3	Sumatra, Indonesia	Mixed secondary forest	59.04 ± 17.15	39.26–69.79	Ketterings et al. (2001)
4	Kampong Thom, Cambodia	Regrowth forest	42.00 ± 21.00	22.00–90.00	Ota et al. (2015)
5	Malaysia	Young forests aged 8.5–17 years	63.60 ± 34.93	34.00–118.00	Kho and Jepsen (2015)

Table A4. Comparing estimated aboveground biomass (AGB; Mg ha^{-1}) in cashew plantations (CPs) using adopted allometric equations (AGB_f), the diameter at breast height (DBH) and tree height (H) power-law relationship (AGB_h), and previous AGB reported in previous studies. Mean ± SD is the mean plus or minus 1 standard deviation.

No.	Region	Vegetation type	AGB (Mg ha^{-1})		References
			Mean ± SD	Range	
1	Kulen, Cambodia	Family-scale cashew plantation	16.70 ± 4.80	11.23–20.23	AGB_h in this study
2	Kulen, Cambodia	Family-scale cashew plantation	70.60 ± 22.01	46.16–88.87	AGB_f in this study
3	Benin	Cashew agroforestry farming	18.07 ± 2.14	–	Biah et al. (2018)
4	Guinean, Côte d'Ivoire	Cashew plantation	13.78 ± 0.98	–	Kanmegne Tamga et al. (2022)
5	Kampong Cham, Cambodia	Large-scale and intensively managed cashew plantation (10–16 years of age)	104.30 ± 19.65	72.00–143.00	Avtar et al. (2013)

Data availability. All the collected data used in this study are publicly available as follows:

1. The datasets of the forest inventory, leaf area index, and leaf functional traits across various land-cover classes are available at https://doi.org/10.5281/zenodo.10146582 (Sovann et al., 2024a).
2. The daily data, including fPAR, soil conditions, and meteorological conditions from 10 April 2022 to 9 April 2023, can be downloaded from https://doi.org/10.5281/zenodo.10159726 (Sovann et al., 2024b).
3. Meteorological data from 10 April 2022 to 9 April 2024 in Kulen, Cambodia, are available at https://doi.org/10.5281/zenodo.13756906 (Sovann et al., 2024c).
4. Future data from the field site will be uploaded to https://zenodo.org/communities/cambodia_ecosystem_data (last access: 10 September 2025) on a regular basis.

Supplement. The supplement related to this article is available online at https://doi.org/10.5194/bg-22-4649-2025-supplement.

Author contributions. CS led field data collection, analysis, and article writing. TT and SO contributed to conceptualization, article review, editing, and supervision. SKo and SS provided administrative support and supervised fieldwork in Cambodia. PV offered technical guidance and support in equipment installation and maintenance. SKi managed field data collection. All authors contributed to editing the article.

Competing interests. The contact author has declared that none of the authors has any competing interests.

Disclaimer. Publisher's note: Copernicus Publications remains neutral with regard to jurisdictional claims made in the text, published maps, institutional affiliations, or any other geographical representation in this paper. While Copernicus Publications makes every effort to include appropriate place names, the final responsibility lies with the authors.

Acknowledgements. We are grateful to the Ministry of Environment (Cambodia) and Siem Reap Provincial Administration for their grant permissions, administrative support, and accommodation during our fieldwork. A special note of thanks goes to Seng Saingheat for his dedication and leadership, along with his ranger colleagues, including Sou Sy, Let Chey, Khun Chi, Soun Sao, Kroem Veng, Choun Choy, and Ti Has. We express our sincere appreciation to the research teams from the Royal University of Agriculture (Cambodia), namely Horn Sarun, Yorn Chomroeun, Sok Pheak, Sum Dara, and Long Sotheara, for their invaluable support in forest inventory. We greatly appreciate Mot Ly and Chim Lychheng, as well as Rum Pheara, Svay Chanboth, and Mach Sokmean, for their support throughout our data collection journey.

Financial support. This work was supported by the Swedish International Development Cooperation Agency through the Sweden–Royal University of Phnom Penh Bilateral programme (grant no. 11599). Torbern Tagesson was additionally funded by the Swedish National Space Agency (SNSA; grant no. 2021-00144) and Formas (grant nos. 2021-00644 and 2023-02436). We also acknowledge funding from Fysiografen. The research presented in this paper is a contribution to the Strategic Research Area "Biodiversity and Ecosystem Services in a Changing Climate", BECC, funded by the Swedish government.

The publication of this article was funded by the Swedish Research Council, Forte, Formas, and Vinnova.

Review statement. This paper was edited by Paul Stoy and reviewed by three anonymous referees.

References

Akossou, A. Y. J., Salifou, A. D., Tchiwanou, L. A., Assani Saliou, S. A., and Azoua, M. H.: Area and Dry Mass Estimation of Cashew (Anacardium Occidentale) Leaves: Effect of Tree Position within a Plantation around Parakou, Benin, Journal of Experimental Agriculture International, 15, 1–12, https://doi.org/10.9734/JEAI/2017/29798, 2016.

Akram, M. A., Wang, X., Shrestha, N., Zhang, Y., Sun, Y., Yao, S., Li, J., Hou, Q., Hu, W., Ran, J., and Deng, J.: Variations and Driving Factors of Leaf Functional Traits in the Dominant Desert Plant Species Along an Environmental Gradient in the Drylands of China, Sci. Total Environ., 897, 165394, https://doi.org/10.1016/j.scitotenv.2023.165394, 2023.

Ali, A., Yan, E. R., Chang, S. X., Cheng, J. Y., and Liu, X. Y.: Community-Weighted Mean of Leaf Traits and Divergence of Wood Traits Predict Aboveground Biomass in Secondary Subtropical Forests, Sci. Total Environ., 574, 654–662, https://doi.org/10.1016/j.scitotenv.2016.09.022, 2017.

Austin, A. T., Yahdjian, L., Stark, J. M., Belnap, J., Porporato, A., Norton, U., Ravetta, D. A., and Schaeffer, S. M.: Water Pulses and Biogeochemical Cycles in Arid and Semiarid Ecosystems, Oecologia, 141, 221–235, https://doi.org/10.1007/s00442-004-1519-1, 2004.

Avtar, R., Takeuchi, W., and Sawada, H.: Monitoring of Biophysical Parameters of Cashew Plants in Cambodia Using Alos/Palsar Data, Environ. Monit. Assess., 185, 2023–2037, https://doi.org/10.1007/s10661-012-2685-y, 2013.

Avtar, R., Suzuki, R., and Sawada, H.: Natural Forest Biomass Estimation Based on Plantation Information Using Palsar Data, PLoS One, 9, e86121, https://doi.org/10.1371/journal.pone.0086121, 2014.

Baker, T. R., Honorio Coronado, E. N., Phillips, O. L., Martin, J., van der Heijden, G. M. F., Garcia, M., and Silva Espejo, J.: Low Stocks of Coarse Woody Debris in a Southwest Amazonian Forest, Oecologia, 152, 495–504, https://doi.org/10.1007/s00442-007-0667-5, 2007.

Barlow, J., Lennox, G. D., Ferreira, J., Berenguer, E., Lees, A. C., Mac Nally, R., Thomson, J. R., Ferraz, S. F., Louzada, J., Oliveira, V. H., Parry, L., Solar, R. R., Vieira, I. C., Aragao, L.

E., Begotti, R. A., Braga, R. F., Cardoso, T. M., de Oliveira, R. C., Jr., Souza, C. M., Jr., Moura, N. G., Nunes, S. S., Siqueira, J. V., Pardini, R., Silveira, J. M., Vaz-de-Mello, F. Z., Veiga, R. C., Venturieri, A., and Gardner, T. A.: Anthropogenic Disturbance in Tropical Forests Can Double Biodiversity Loss from Deforestation, Nature, 535, 144–147, https://doi.org/10.1038/nature18326, 2016.

Bezerra, M. A., Lacerda, C. F. D., Gomes Filho, E., Abreu, C. E. B. D., and Prisco, J. T.: Physiology of Cashew Plants Grown under Adverse Conditions, Brazilian Journal of Plant Physiology, 19, 449–461, https://doi.org/10.1590/s1677-04202007000400012, 2007.

Bhandari, S. K., Veneklaas, E. J., McCaw, L., Mazanec, R., Whitford, K., and Renton, M.: Effect of thinning and fertilizer on growth and allometry of *Eucalyptus marginata*, Forest Ecol. Manag., 479, 118594, https://doi.org/10.1016/j.foreco.2020.118594, 2021.

Biah, I., Guendehou, S., Goussanou, C., Kaire, M., and Sinsin, B. A.: Allometric Models for Estimating Biomass Stocks in Cashew (Anacardium Occidentale L.) Plantation in Benin, Bulletin de la Recherche Agronomique du Bénin, 84, 16–27, 2018.

Brown, S.: Estimating Biomass and Biomass Change of Tropical Forests: A Primer, Food and Agriculture Organization of the United Nations, ISBN 92-5-103955-0, https://www.fao.org/4/w4095e/w4095e00.htm, 1997.

Burt, A., Calders, K., Cuni-Sanchez, A., Gómez-Dans, J., Lewis, P., Lewis, S. L., Malhi, Y., Phillips, O. L., and Disney, M.: Assessment of Bias in Pan-Tropical Biomass Predictions, Front. For. Glob. Change, 3, https://doi.org/10.3389/ffgc.2020.00012, 2020.

Cardinale, B. J., Duffy, J. E., Gonzalez, A., Hooper, D. U., Perrings, C., Venail, P., Narwani, A., Mace, G. M., Tilman, D., Wardle, D. A., Kinzig, A. P., Daily, G. C., Loreau, M., Grace, J. B., Larigauderie, A., Srivastava, D. S., and Naeem, S.: Biodiversity Loss and Its Impact on Humanity, Nature, 486, 59–67, https://doi.org/10.1038/nature11148, 2012.

Chave, J., Andalo, C., Brown, S., Cairns, M. A., Chambers, J. Q., Eamus, D., Folster, H., Fromard, F., Higuchi, N., Kira, T., Lescure, J. P., Nelson, B. W., Ogawa, H., Puig, H., Riera, B., and Yamakura, T.: Tree Allometry and Improved Estimation of Carbon Stocks and Balance in Tropical Forests, Oecologia, 145, 87–99, https://doi.org/10.1007/s00442-005-0100-x, 2005.

Chave, J., Rejou-Mechain, M., Burquez, A., Chidumayo, E., Colgan, M. S., Delitti, W. B., Duque, A., Eid, T., Fearnside, P. M., Goodman, R. C., Henry, M., Martinez-Yrizar, A., Mugasha, W. A., Muller-Landau, H. C., Mencuccini, M., Nelson, B. W., Ngomanda, A., Nogueira, E. M., Ortiz-Malavassi, E., Pelissier, R., Ploton, P., Ryan, C. M., Saldarriaga, J. G., and Vieilledent, G.: Improved Allometric Models to Estimate the Aboveground Biomass of Tropical Trees, Glob. Change Biol., 20, 3177–3190, https://doi.org/10.1111/gcb.12629, 2014.

Chen, B. Q., Li, X. P., Xiao, X. M., Zhao, B., Dong, J. W., Kou, W. L., Qin, Y. W., Yang, C., Wu, Z. X., Sun, R., Lan, G. Y., and Xie, G. S.: Mapping Tropical Forests and Deciduous Rubber Plantations in Hainan Island, China by Integrating Palsar 25-M and Multi-Temporal Landsat Images, Int. J. Appl. Earth Obs., 50, 117–130, https://doi.org/10.1016/j.jag.2016.03.011, 2016.

Chheng, K., Sasaki, N., Mizoue, N., Khorn, S., Kao, D., and Lowe, A.: Assessment of Carbon Stocks of Semi-Evergreen Forests in Cambodia, Global Ecology and Conservation, 5, 34–47, https://doi.org/10.1016/j.gecco.2015.11.007, 2016.

Chim, K., Tunnicliffe, J., Shamseldin, A., and Ota, T.: Land Use Change Detection and Prediction in Upper Siem Reap River, Cambodia, Hydrology, 6, 64, https://doi.org/10.3390/hydrology6030064, 2019.

Chim, K., Tunnicliffe, J., Shamseldin, A., and Sarun, S.: Sustainable Water Management in the Angkor Temple Complex, Cambodia, SN Appl. Sci., 3, 74, https://doi.org/10.1007/s42452-020-04030-0, 2021.

Clark, D. B., Oberbauer, S. F., Clark, D. A., Ryan, M. G., and Dubayah, R. O.: Physical Structure and Biological Composition of Canopies in Tropical Secondary and Old-Growth Forests, PLoS One, 16, e0256571, https://doi.org/10.1371/journal.pone.0256571, 2021.

Con, T. V., Thang, N. T., Ha, D. T. T., Khiem, C. C., Quy, T. H., Lam, V. T., Van Do, T., and Sato, T.: Relationship between Aboveground Biomass and Measures of Structure and Species Diversity in Tropical Forests of Vietnam, Forest Ecol. Manag., 310, 213–218, https://doi.org/10.1016/j.foreco.2013.08.034, 2013.

Coste, S., Baraloto, C., Leroy, C., Marcon, É., Renaud, A., Richardson, A. D., Roggy, J. C., Schimann, H., Uddling, J., and Hérault, B.: Assessing Foliar Chlorophyll Contents with the Spad-502 Chlorophyll Meter: A Calibration Test with Thirteen Tree Species of Tropical Rainforest in French Guiana, Ann. For. Sci., 67, 607–607, https://doi.org/10.1051/forest/2010020, 2010.

Dawson, T. P., North, P. R. J., Plummer, S. E., and Curran, P. J.: Forest Ecosystem Chlorophyll Content: Implications for Remotely Sensed Estimates of Net Primary Productivity, Int. J. Remote Sens., 24, 611–617, https://doi.org/10.1080/01431160304984, 2003.

Deng, C., Zhang, S. G., Lu, Y. C., Froese, R. E., Ming, A. G., and Li, Q. F.: Thinning Effects on the Tree Height–Diameter Allometry of Masson Pine (Pinus Massoniana Lamb.), Forests, 10, 1129, https://doi.org/10.3390/f10121129, 2019.

Díaz, S., Lavorel, S., De Bello, F., Quétier, F., Grigulis, K., and Robson, T. M.: Incorporating Plant Functional Diversity Effects in Ecosystem Service Assessments, P. Natl. Acad. Sci. USA, 104, 20684–20689, https://doi.org/10.1073/pnas.0704716104, 2007.

Fan, F., Li, W., Feng, Z., and Yang, Y.: Combining Landscape Patterns and Ecosystem Services to Disclose Ecosystem Changes in Tropical Cropland-Forest Shifting Zones: Inspiration from Mainland Southeast Asia, J. Clean. Prod., 434, 140058, https://doi.org/10.1016/j.jclepro.2023.140058, 2024.

Fang, H., Baret, F., Plummer, S., and Schaepman-Strub, G.: An Overview of Global Leaf Area Index (Lai): Methods, Products, Validation, and Applications, Rev. Geophys., 57, 739–799, https://doi.org/10.1029/2018RG000608, 2019.

Feldpausch, T. R., Banin, L., Phillips, O. L., Baker, T. R., Lewis, S. L., Quesada, C. A., Affum-Baffoe, K., Arets, E. J. M. M., Berry, N. J., Bird, M., Brondizio, E. S., de Camargo, P., Chave, J., Djagbletey, G., Domingues, T. F., Drescher, M., Fearnside, P. M., França, M. B., Fyllas, N. M., Lopez-Gonzalez, G., Hladik, A., Higuchi, N., Hunter, M. O., Iida, Y., Salim, K. A., Kassim, A. R., Keller, M., Kemp, J., King, D. A., Lovett, J. C., Marimon, B. S., Marimon-Junior, B. H., Lenza, E., Marshall, A. R., Metcalfe, D. J., Mitchard, E. T. A., Moran, E. F., Nelson, B. W., Nilus, R., Nogueira, E. M., Palace, M., Patiño, S., Peh, K. S.-H., Raven-

tos, M. T., Reitsma, J. M., Saiz, G., Schrodt, F., Sonké, B., Taedoumg, H. E., Tan, S., White, L., Wöll, H., and Lloyd, J.: Height-diameter allometry of tropical forest trees, Biogeosciences, 8, 1081–1106, https://doi.org/10.5194/bg-8-1081-2011, 2011.

Feng, X., Uriarte, M., Gonzalez, G., Reed, S., Thompson, J., Zimmerman, J. K., and Murphy, L.: Improving Predictions of Tropical Forest Response to Climate Change through Integration of Field Studies and Ecosystem Modeling, Glob. Change Biol., 24, e213–e232, https://doi.org/10.1111/gcb.13863, 2018.

Fichtner, A. and Härdtle, W.: Forest Ecosystems: A Functional and Biodiversity Perspective, in: Perspectives for Biodiversity and Ecosystems, Environmental Challenges and Solutions, Springer International Publishing, 383–405, https://doi.org/10.1007/978-3-030-57710-0_16, 2021.

Finegan, B., Peña-Claros, M., de Oliveira, A., Ascarrunz, N., Bret-Harte, M. S., Carreño-Rocabado, G., Casanoves, F., Díaz, S., Eguiguren Velepucha, P., Fernandez, F., Licona, J. C., Lorenzo, L., Salgado Negret, B., Vaz, M., and Poorter, L.: Does Functional Trait Diversity Predict above-Ground Biomass and Productivity of Tropical Forests? Testing Three Alternative Hypotheses, J. Ecol., 103, 191–201, https://doi.org/10.1111/1365-2745.12346, 2015.

Forrester, D. I., Baker, T. G., Elms, S. R., Hobi, M. L., Ouyang, S., Wiedemann, J. C., Xiang, W., Zell, J., and Pulkkinen, M.: Self-Thinning Tree Mortality Models That Account for Vertical Stand Structure, Species Mixing and Climate, Forest Ecol. Manag., 487, 118936, https://doi.org/10.1016/j.foreco.2021.118936, 2021.

Galanes, I. T. and Thomlinson, J. R.: Relationships between Spatial Configuration of Tropical Forest Patches and Woody Plant Diversity in Northeastern Puerto Rico, Plant Ecol., 201, 101–113, https://doi.org/10.1007/s11258-008-9475-1, 2009.

Gamon, J. A., Coburn, C., Flanagan, L. B., Huemmrich, K. F., Kiddle, C., Sanchez-Azofeifa, G. A., Thayer, D. R., Vescovo, L., Gianelle, D., Sims, D. A., Rahman, A. F., and Pastorello, G. Z.: Specnet Revisited: Bridging Flux and Remote Sensing Communities, Can. J. Remote Sens., 36, S376–S390, https://doi.org/10.5589/m10-067, 2010.

Gao, J., Wang, K., and Zhang, X.: Patterns and Drivers of Community Specific Leaf Area in China, Global Ecology and Conservation, 33, e01971, https://doi.org/10.1016/j.gecco.2021.e01971, 2022.

Gao, W.-Q., Lei, X.-D., Gao, D.-L., and Li, Y.-T.: Mass-Ratio and Complementarity Effects Simultaneously Drive Aboveground Biomass in Temperate *Quercus* Forests through Stand Structure, Ecol. Evol., 11, 16806–16816, https://doi.org/10.1002/ece3.8312, 2021.

Gardner, T. A., Barlow, J., Chazdon, R., Ewers, R. M., Harvey, C. A., Peres, C. A., and Sodhi, N. S.: Prospects for Tropical Forest Biodiversity in a Human-Modified World, Ecol. Lett., 12, 561–582, https://doi.org/10.1111/j.1461-0248.2009.01294.x, 2009.

Garnier, E., Shipley, B., Roumet, C., and Laurent, G.: A Standardized Protocol for the Determination of Specific Leaf Area and Leaf Dry Matter Content, Funct. Ecol., 15, 688–695, https://doi.org/10.1046/j.0269-8463.2001.00563.x, 2001.

Garnier, E., Cortez, J., Billès, G., Navas, M. L., Roumet, C., Debussche, M., Laurent, G., Blanchard, A., Aubry, D., Bellmann, A., Neill, C., and Toussaint, J. P.: Plant Functional Markers Capture Ecosystem Properties during Secondary Succession, Ecology, 85, 2630–2637, https://doi.org/10.1890/03-0799, 2004.

Gea-Izquierdo, G. and Sánchez-González, M.: Forest Disturbances and Climate Constrain Carbon Allocation Dynamics in Trees, Glob. Change Biol., 28, 4342–4358, https://doi.org/10.1111/gcb.16172, 2022.

Geissler, P., Hartmann, T., Ihlow, F., Neang, T., Seng, R., Wagner, P., and Böhme, W.: Herpetofauna of the Phnom Kulen National Park, Northern Cambodia—An Annotated Checklist, Cambodian Journal of Natural History, 2019, 40–63, 2019.

Geng, J., Li, H., Pang, J., Zhang, W., and Shi, Y.: The Effects of Land-Use Conversion on Evapotranspiration and Water Balance of Subtropical Forest and Managed Tea Plantation in Taihu Lake Basin, China, 36, e14652, https://doi.org/10.1002/hyp.14652, 2022.

Giam, X.: Global Biodiversity Loss from Tropical Deforestation, P. Natl. Acad. Sci. USA, 114, 5775–5777, https://doi.org/10.1073/pnas.1706264114, 2017.

Gloor, M., Brienen, R. J. W., Galbraith, D., Feldpausch, T. R., Schöngart, J., Guyot, J. L., Espinoza, J. C., Lloyd, J., and Phillips, O. L.: Intensification of the Amazon Hydrological Cycle over the Last Two Decades, Geophys. Res. Lett., 40, 1729–1733, https://doi.org/10.1002/grl.50377, 2013.

Green, J. K., Berry, J., Ciais, P., Zhang, Y., and Gentine, P.: Amazon Rainforest Photosynthesis Increases in Response to Atmospheric Dryness, Sci. Adv., 6, eabb7232, https://doi.org/10.1126/sciadv.abb7232, 2020.

Grogan, K., Pflugmacher, D., Hostert, P., Kennedy, R., and Fensholt, R.: Cross-Border Forest Disturbance and the Role of Natural Rubber in Mainland Southeast Asia Using Annual Landsat Time Series, Remote Sens. Environ., 169, 438–453, https://doi.org/10.1016/j.rse.2015.03.001, 2015.

Guerrieri, R., Correia, M., Martín-Forés, I., Alfaro-Sánchez, R., Pino, J., Hampe, A., Valladares, F., and Espelta, J. M.: Land-Use Legacies Influence Tree Water-Use Efficiency and Nitrogen Availability in Recently Established European Forests, Funct. Ecol., 35, 1325–1340, https://doi.org/10.1111/1365-2435.13787, 2021.

Guo, H., Duan, D., Lei, H., Chen, Y., Li, J., Albasher, G., and Li, X.: Environmental Drivers of Landscape Fragmentation Influence Intraspecific Leaf Traits in Forest Ecosystem, Forests, 14, 1875, https://doi.org/10.3390/f14091875, 2023a.

Guo, J., Feng, H., McNie, P., Liu, Q., Xu, X., Pan, C., Yan, K., Feng, L., Adehanom Goitom, E., and Yu, Y.: Species Mixing Improves Soil Properties and Enzymatic Activities in Chinese Fir Plantations: A Meta-Analysis, CATENA, 220, 106723, https://doi.org/10.1016/j.catena.2022.106723, 2023b.

Ha, V.: Forest Fragmentation in Vietnam: Effects on Tree Diversity, Populations and Genetics, Ph.D. thesis, Utrecht University, the Netherlands, 114 pp., ISBN 978-90-393-6351-5, https://research-portal.uu.nl/files/12699324/VanTiep.pdf, 2015.

Hang, P., Ishwaran, N., Hong, T., and Delanghe, P.: From Conservation to Sustainable Development – a Case Study of Angkor World Heritage Site, Cambodia, Journal of Environmental Science and Engineering A, ISSN 2162-5298, ISSN 2162-5301, David Publishing Company, 5, 141–155, http://www.davidpublisher.com/Home/Journal/JESE-A, https://doi.org/10.17265/2162-5298/2016.03.004, 2016.

Hansen, M. C., Potapov, P. V., Moore, R., Hancher, M., Turubanova, S. A., Tyukavina, A., Thau, D., Stehman, S. V., Goetz, S. J., Loveland, T. R., Kommareddy, A., Egorov, A., Chini, L., Justice, C. O., and Townshend, J. R.: High-Resolution Global Maps of 21st-Century Forest Cover Change, Science, 342, 850–853, https://doi.org/10.1126/science.1244693, 2013.

He, L. M., Wang, R., Mostovoy, G., Liu, J. E., Chen, J. M., Shang, J. L., Liu, J. G., McNairn, H., and Powers, J.: Crop Biomass Mapping Based on Ecosystem Modeling at Regional Scale Using High Resolution Sentinel-2 Data, Remote Sensing, 13, 806, https://doi.org/10.3390/rs13040806, 2021.

Hector, A.: The Effect of Diversity on Productivity: Detecting the Role of Species Complementarity, Oikos, 82, 597–599, https://doi.org/10.2307/3546380, 1998.

Hill, M. O.: Diversity and Evenness: A Unifying Notation and Its Consequences, Ecology, 54, 427–432, https://doi.org/10.2307/1934352, 1973.

Horel, Á., Zsigmond, T., Molnár, S., Zagyva, I., and Bakacsi, Z.: Long-Term Soil Water Content Dynamics under Different Land Uses in a Small Agricultural Catchment, J. Hydrol. Hydromech., 70, 284–294, https://doi.org/10.2478/johh-2022-0015, 2022.

Howell, S. R., Song, G.-Z. M., Chao, K.-J., Doley, D., and Camac, J.: Functional Evaluation of Height–Diameter Relationships and Tree Development in an Australian Subtropical Rainforest, Aust. J. Bot., 70, 158–173, https://doi.org/10.1071/bt21049, 2022.

Huxley, J.: Problems of Relative Growth, L. MacVeagh, The Dial Press, New York, https://doi.org/10.5962/bhl.title.6427, 1932.

Ibrahim, H. M. and Alghamdi, A. G.: Effect of the Particle Size of Clinoptilolite Zeolite on Water Content and Soil Water Storage in a Loamy Sand Soil, Water, 13, 607, https://doi.org/10.3390/w13050607, 2021.

International Council for Research in Agroforestry (ICRAF): Tree Functional Attributes and Ecological Database [data set], http://db.worldagroforestry.org/ (last access: 21 May 2022), 2022.

Ito, E., Khorn, S., Lim, S., Pol, S., Tith, B., Pith, P., Tani, A., Kanzaki, M., Kaneko, T., Okuda, Y., Kabeya, N., Nobuhiro, T., and Araki, M.: Comparison of the Leaf Area Index (Lai) of Two Types of Dipterocarp Forest on the West Bank of the Mekong River, Cambodia, in: Forest Environments in the Mekong River Basin, Phnom Penh, Cambodia, 5–7 December 2005, 214–221, https://www.ffpri.go.jp/labs/cwcm/event/IUFRO2005.pdf, https://doi.org/10.1007/978-4-431-46503-4_19, 2007.

Jacobson, C., Smith, J., Sou, S., Nielsen, C., and Hang, P.: Effective Water Management for Landscape Management in the Siem Reap Catchment, Cambodia, in: Biodiversity-Health-Sustainability Nexus in Socio-Ecological Production Landscapes and Seascapes (Sepls), Satoyama Initiative Thematic Review, Springer Nature Singapore, 129–150, https://doi.org/10.1007/978-981-16-9893-4_7, 2022.

Jactel, H., Gritti, E. S., Drossler, L., Forrester, D. I., Mason, W. L., Morin, X., Pretzsch, H., and Castagneyrol, B.: Positive Biodiversity-Productivity Relationships in Forests: Climate Matters, Biol. Lett., 14, 20170747, https://doi.org/10.1098/rsbl.2017.0747, 2018.

Johansson, E., Olin, S., and Seaquist, J.: Foreign Demand for Agricultural Commodities Drives Virtual Carbon Exports from Cambodia, Environ. Res. Lett., 15, 064034, https://doi.org/10.1088/1748-9326/ab8157, 2020.

Kanmegne Tamga, D., Latifi, H., Ullmann, T., Baumhauer, R., Bayala, J., and Thiel, M.: Estimation of Aboveground Biomass in Agroforestry Systems over Three Climatic Regions in West Africa Using Sentinel-1, Sentinel-2, Alos, and Gedi Data, Sensors (Basel), 23, 349, https://doi.org/10.3390/s23010349, 2022.

Kattge, J., Bonisch, G., Diaz, S., et al.: Try Plant Trait Database – Enhanced Coverage and Open Access, Glob. Change Biol., 26, 119–188, https://doi.org/10.1111/gcb.14904, 2020.

Kennedy, R. E., Yang, Z., Gorelick, N., Braaten, J., Cavalcante, L., Cohen, W. B., and Healey, S.: Implementation of the Landtrendr Algorithm on Google Earth Engine, Remote Sens., 10, 691, https://doi.org/10.3390/rs10050691, 2018.

Kenzo, T., Ichie, T., Hattori, D., Itioka, T., Handa, C., Ohkubo, T., Kendawang, J. J., Nakamura, M., Sakaguchi, M., Takahashi, N., Okamoto, M., Tanaka-Oda, A., Sakurai, K., and Ninomiya, I.: Development of Allometric Relationships for Accurate Estimation of above- and Below-Ground Biomass in Tropical Secondary Forests in Sarawak, Malaysia, J. Trop. Ecol., 25, 371–386, https://doi.org/10.1017/S0266467409006129, 2009.

Ketterings, Q. M., Coe, R., van Noordwijk, M., Ambagau, Y., and Palm, C. A.: Reducing Uncertainty in the Use of Allometric Biomass Equations for Predicting above-Ground Tree Biomass in Mixed Secondary Forests, Forest Ecol. Manag., 146, 199–209, https://doi.org/10.1016/S0378-1127(00)00460-6, 2001.

Kho, L. K. and Jepsen, M. R.: Carbon Stock of Oil Palm Plantations and Tropical Forests in Malaysia: A Review, Singapore J. Trop. Geogr., 36, 249–266, https://doi.org/10.1111/sjtg.12100, 2015.

Kim, S., Horn, S., Sok, P., Sien, T., and Yorn, C.: Ecosystem Carbon Stock Assessment in Upland Forest: A Case Study in Koh Kong, Mondulkiri, Preah Vihear, and Siem Reap Provinces, Environmental and Rural Development, 14, 61–67, https://doi.org/10.32115/ijerd.14.2_61, 2023.

King, D. A., Davies, S. J., Tan, S., and Noor, N. S. M.: The Role of Wood Density and Stem Support Costs in the Growth and Mortality of Tropical Trees, J. Ecol., 94, 670–680, https://doi.org/10.1111/j.1365-2745.2006.01112.x, 2006.

Kiyono, Y., Ochiai, Y., Chiba, Y., Asai, H., Saito, K., Shiraiwa, T., Horie, T., Songnoukhai, V., Navongxai, V., and Inoue, Y.: Predicting Chronosequential Changes in Carbon Stocks of Pachymorph Bamboo Communities in Slash-and-Burn Agricultural Fallow, Northern Lao People's Democratic Republic, Journal of Forest Research, 12, 371–383, https://doi.org/10.1007/s10310-007-0028-6, 2007.

Kiyono, Y., Ito, E., Monda, Y., Toriyama, J., and Sum, T.: Effects of Large Aboveground Biomass Loss Events on the Deadwood and Litter Mass Dynamics of Seasonal Tropical Forests in Cambodia, Tropics, 27, 33–48, https://doi.org/10.3759/tropics.MS18-05, 2018.

Kramer, J. M. F., Zwiener, V. P., and Müller, S. C.: Biotic Homogenization and Differentiation of Plant Communities in Tropical and Subtropical Forests, Conserv. Biol., 37, e14025, https://doi.org/10.1111/cobi.14025, 2023.

Kumaresh, V., Rani, M. S. A., Vethamoni, P. I., Senthil, A., and Uma, D.: Morphological and Physiological Analysis of Vri-3 Cashew Plantations under Different Planting Density Systems, International Journal of Environment and Climate Change, 13, 3698–3706, https://doi.org/10.9734/ijecc/2023/v13i103041, 2023.

Laurance, W. F., Sayer, J., and Cassman, K. G.: Agricultural Expansion and Its Impacts on Tropical Nature, Trends Ecol. Evol., 29, 107–116, https://doi.org/10.1016/j.tree.2013.12.001, 2014.

Laurans, M., Hérault, B., Vieilledent, G., and Vincent, G.: Vertical Stratification Reduces Competition for Light in Dense Tropical Forests, Forest Ecol. Manag., 329, 79–88, https://doi.org/10.1016/j.foreco.2014.05.059, 2014.

Leoni, E., Altesor, A., and Paruelo, J. M.: Explaining Patterns of Primary Production from Individual Level Traits, J. Veg. Sci., 20, 612–619, https://doi.org/10.1111/j.1654-1103.2009.01080.x, 2009.

Lewis, S. L., Sonke, B., Sunderland, T., Begne, S. K., Lopez-Gonzalez, G., van der Heijden, G. M., Phillips, O. L., Affum-Baffoe, K., Baker, T. R., Banin, L., Bastin, J. F., Beeckman, H., Boeckx, P., Bogaert, J., De Canniere, C., Chezeaux, E., Clark, C. J., Collins, M., Djagbletey, G., Djuikouo, M. N., Droissart, V., Doucet, J. L., Ewango, C. E., Fauset, S., Feldpausch, T. R., Foli, E. G., Gillet, J. F., Hamilton, A. C., Harris, D. J., Hart, T. B., de Haulleville, T., Hladik, A., Hufkens, K., Huygens, D., Jeanmart, P., Jeffery, K. J., Kearsley, E., Leal, M. E., Lloyd, J., Lovett, J. C., Makana, J. R., Malhi, Y., Marshall, A. R., Ojo, L., Peh, K. S., Pickavance, G., Poulsen, J. R., Reitsma, J. M., Sheil, D., Simo, M., Steppe, K., Taedoumg, H. E., Talbot, J., Taplin, J. R., Taylor, D., Thomas, S. C., Toirambe, B., Verbeeck, H., Vleminckx, J., White, L. J., Willcock, S., Woell, H., and Zemagho, L.: Above-Ground Biomass and Structure of 260 African Tropical Forests, Philos. Trans. R. Soc. Lond. B Biol. Sci., 368, 20120295, https://doi.org/10.1098/rstb.2012.0295, 2013.

Li, Y., Liu, C., Zhang, J., Yang, H., Xu, L., Wang, Q., Sack, L., Wu, X., Hou, J., and He, N.: Variation in Leaf Chlorophyll Concentration from Tropical to Cold-Temperate Forests: Association with Gross Primary Productivity, Ecol. Indic., 85, 383–389, https://doi.org/10.1016/j.ecolind.2017.10.025, 2018.

Liang, J., Crowther, T. W., Picard, N., Wiser, S., Zhou, M., Alberti, G., Schulze, E. D., McGuire, A. D., Bozzato, F., Pretzsch, H., de-Miguel, S., Paquette, A., Herault, B., Scherer-Lorenzen, M., Barrett, C. B., Glick, H. B., Hengeveld, G. M., Nabuurs, G. J., Pfautsch, S., Viana, H., Vibrans, A. C., Ammer, C., Schall, P., Verbyla, D., Tchebakova, N., Fischer, M., Watson, J. V., Chen, H. Y., Lei, X., Schelhaas, M. J., Lu, H., Gianelle, D., Parfenova, E. I., Salas, C., Lee, E., Lee, B., Kim, H. S., Bruelheide, H., Coomes, D. A., Piotto, D., Sunderland, T., Schmid, B., Gourlet-Fleury, S., Sonke, B., Tavani, R., Zhu, J., Brandl, S., Vayreda, J., Kitahara, F., Searle, E. B., Neldner, V. J., Ngugi, M. R., Baraloto, C., Frizzera, L., Balazy, R., Oleksyn, J., Zawila-Niedzwiecki, T., Bouriaud, O., Bussotti, F., Finer, L., Jaroszewicz, B., Jucker, T., Valladares, F., Jagodzinski, A. M., Peri, P. L., Gonmadje, C., Marthy, W., O'Brien, T., Martin, E. H., Marshall, A. R., Rovero, F., Bitariho, R., Niklaus, P. A., Alvarez-Loayza, P., Chamuya, N., Valencia, R., Mortier, F., Wortel, V., Engone-Obiang, N. L., Ferreira, L. V., Odeke, D. E., Vasquez, R. M., Lewis, S. L., and Reich, P. B.: Positive Biodiversity-Productivity Relationship Predominant in Global Forests, Science, 354, aaf8957–aaf8957, https://doi.org/10.1126/science.aaf8957, 2016.

Liu, Z., Zhao, M., Zhang, H., Ren, T., Liu, C., and He, N.: Divergent Response and Adaptation of Specific Leaf Area to Environmental Change at Different Spatio-Temporal Scales Jointly Improve Plant Survival, Glob. Change Biol., 29, 1144–1159, https://doi.org/10.1111/gcb.16518, 2023.

Luo, Z., Niu, J., He, S., Zhang, L., Chen, X., Tan, B., Wang, D., and Berndtsson, R.: Linking Roots, Preferential Flow, and Soil Moisture Redistribution in Deciduous and Coniferous Forest Soils, J. Soil. Sediment., 23, 1524–1538, https://doi.org/10.1007/s11368-022-03375-w, 2023.

Lutz, J. A., Furniss, T. J., Johnson, D. J., Davies, S. J., Allen, D., Alonso, A., Anderson-Teixeira, K. J., Andrade, A., Baltzer, J., Becker, K. M. L., Blomdahl, E. M., Bourg, N. A., Bunyavejchewin, S., Burslem, D. F. R. P., Cansler, C. A., Cao, K., Cao, M., Cárdenas, D., Chang, L. W., Chao, K. J., Chao, W. C., Chiang, J. M., Chu, C., Chuyong, G. B., Clay, K., Condit, R., Cordell, S., Dattaraja, H. S., Duque, A., Ewango, C. E. N., Fischer, G. A., Fletcher, C., Freund, J. A., Giardina, C., Germain, S. J., Gilbert, G. S., Hao, Z., Hart, T., Hau, B. C. H., He, F., Hector, A., Howe, R. W., Hsieh, C. F., Hu, Y. H., Hubbell, S. P., Inman-Narahari, F. M., Itoh, A., Janík, D., Kassim, A. R., Kenfack, D., Korte, L., Král, K., Larson, A. J., Li, Y., Lin, Y., Liu, S., Lum, S., Ma, K., Makana, J. R., Malhi, Y., McMahon, S. M., McShea, W. J., Memiaghe, H. R., Mi, X., Morecroft, M., Musili, P. M., Myers, J. A., Novotny, V., De Oliveira, A., Ong, P., Orwig, D. A., Ostertag, R., Parker, G. G., Patankar, R., Phillips, R. P., Reynolds, G., Sack, L., Song, G. Z. M., Su, S. H., Sukumar, R., Sun, I. F., Suresh, H. S., Swanson, M. E., Tan, S., Thomas, D. W., Thompson, J., Uriarte, M., Valencia, R., Vicentini, A., Vrška, T., Wang, X., Weiblen, G. D., Wolf, A., Wu, S. H., Xu, H., Yamakura, T., Yap, S., and Zimmerman, J. K.: Global Importance of Large-Diameter Trees, Global Ecol. Biogeogr., 27, 849–864, https://doi.org/10.1111/geb.12747, 2018.

Males, J., Artaxo, P., Hansson, H. C., Machado, L. A. T., and Rizzo, L. V.: Tropical Forests Are Crucial in Regulating the Climate on Earth, PLOS Climate, 1, e0000054, https://doi.org/10.1371/journal.pclm.0000054, 2022.

Malimbwi, R. E., Eid, T., and Chamshama, S. A. O.: Allometric Tree Biomass and Volume Models in Tanzania, Department of Forest Mensuration and Management, Sokoine University of Agriculture, Morogoro, Tanzania, 129 pp., ISBN 978-9976-9930-1-1, 2016.

Manuel Villa, P., Ali, A., Venâncio Martins, S., Nolasco de Oliveira Neto, S., Cristina Rodrigues, A., Teshome, M., Alvim Carvalho, F., Heringer, G., and Gastauer, M.: Stand Structural Attributes and Functional Trait Composition Overrule the Effects of Functional Divergence on Aboveground Biomass during Amazon Forest Succession, Forest Ecol. Manag., 477, 118481, https://doi.org/10.1016/j.foreco.2020.118481, 2020.

Maréchaux, I., Bonal, D., Bartlett, M. K., Burban, B., Coste, S., Courtois, E. A., Dulormne, M., Goret, J.-Y., Mira, E., Mirabel, A., Sack, L., Stahl, C., and Chave, J.: Dry-Season Decline in Tree Sapflux Is Correlated with Leaf Turgor Loss Point in a Tropical Rainforest, Funct. Ecol., 32, 2285–2297, https://doi.org/10.1111/1365-2435.13188, 2018.

Matschullat, J.: Save Cambodia's Wildlife: Atlas of Cambodia. Maps on Socio-Economic Development and Environment, Environ. Earth Sci., 72, 1295–1298, https://doi.org/10.1007/s12665-014-3325-3, 2014.

Miettinen, J., Shi, C. H., and Liew, S. C.: Deforestation Rates in Insular Southeast Asia between 2000 and 2010, Glob. Change Biol., 17, 2261–2270, https://doi.org/10.1111/j.1365-2486.2011.02398.x, 2011.

Mlagalila, H. E.: Assessment of Volume, Biomass and Carbon Stock of Cashewnuts Trees in Liwale District, Tanzania, M.Sc. thesis, Sokoine University of Agriculture, Morogoro, Tanzania, 55 pp., https://www.suaire.sua.ac.tz/handle/123456789/1521, 2016.

Mog, B. and Nayak, M. G.: Leaf Morphological and Physiological Traits and Their Significance in Yield Improvement of Fifteen Cashew Varieties in West Coast Region of Karnataka, International Journal of Current Microbiology and Applied Sciences, 7, 1455–1469, https://doi.org/10.20546/ijcmas.2018.707.173, 2018.

Mrad, A., Manzoni, S., Oren, R., Vico, G., Lindh, M., and Katul, G.: Recovering the Metabolic, Self-Thinning, and Constant Final Yield Rules in Mono-Specific Stands, Front. For. Glob. Change, 3, https://doi.org/10.3389/ffgc.2020.00062, 2020.

Naeem, S., Thompson, L. J., Lawler, S. P., Lawton, J. H., and Woodfin, R. M.: Declining Biodiversity Can Alter the Performance of Ecosystems, Nature, 368, 734–737, https://doi.org/10.1038/368734a0, 1994.

Nam, V. T., van Kuijk, M., and Anten, N. P.: Allometric Equations for Aboveground and Belowground Biomass Estimations in an Evergreen Forest in Vietnam, PLoS One, 11, e0156827, https://doi.org/10.1371/journal.pone.0156827, 2016.

Ndiaye, S., Djighaly, P. I., Diarra, A., and Dramé, F. A.: Comparative Study of the Carbon Stock of a Cashew Tree Plantation (Anacardium Occidentale L.) and Secondary Forest in Casamance, Senegal, Nippon Journal of Environmental Science, 1, 1022, https://doi.org/10.46266/njes.1022, 2020.

Nguyen, T. D. and Kappas, M.: Estimating the Aboveground Biomass of an Evergreen Broadleaf Forest in Xuan Lien Nature Reserve, Thanh Hoa, Vietnam, Using Spot-6 Data and the Random Forest Algorithm, International J. Forestry Res., 2020, 1–13, https://doi.org/10.1155/2020/4216160, 2020.

Niinemets, Ü.: A Review of Light Interception in Plant Stands from Leaf to Canopy in Different Plant Functional Types and in Species with Varying Shade Tolerance, Ecol. Res., 25, 693–714, https://doi.org/10.1007/s11284-010-0712-4, 2010.

Nyirambangutse, B., Zibera, E., Uwizeye, F. K., Nsabimana, D., Bizuru, E., Pleijel, H., Uddling, J., and Wallin, G.: Carbon stocks and dynamics at different successional stages in an Afromontane tropical forest, Biogeosciences, 14, 1285–1303, https://doi.org/10.5194/bg-14-1285-2017, 2017.

Nzegbule, E. C., Onyema, M. C., and Ndelekwute, S. C.: Plant Species Richness and Soil Nutrients in a 35-Year Old Cashew Nut Plantation in Isuochi, Southern Nigeria, Tropical Ecology, 54, 205–212, 2013.

Olofsson, P. and Eklundh, L.: Estimation of Absorbed Par across Scandinavia from Satellite Measurements. Part Ii: Modeling and Evaluating the Fractional Absorption, Remote Sens. Environ., 110, 240–251, https://doi.org/10.1016/j.rse.2007.02.020, 2007.

Omuto, C. T., Vargas, R., Viatkin, K., and Yigini, Y. (Eds.): Lesson 4 – Spatial Modeling of Salt-Affected Soils, Global Soil Salinity Map – Gssmap, FAO, Room, Italy, https://openknowledge.fao.org/handle/20.500.14283/ca9209en, 2020.

Ota, T., Ogawa, M., Shimizu, K., Kajisa, T., Mizoue, N., Yoshida, S., Takao, G., Hirata, Y., Furuya, N., Sano, T., Sokh, H., Ma, V., Ito, E., Toriyama, J., Monda, Y., Saito, H., Kiyono, Y., Chann, S., and Ket, N.: Aboveground Biomass Estimation Using Structure from Motion Approach with Aerial Photographs in a Seasonal Tropical Forest, Forests, 6, 3882–3898, https://doi.org/10.3390/f6113882, 2015.

Pan, Y., Birdsey, R. A., Phillips, O. L., Houghton, R. A., Fang, J., Kauppi, P. E., Keith, H., Kurz, W. A., Ito, A., Lewis, S. L., Nabuurs, G.-J., Shvidenko, A., Hashimoto, S., Lerink, B., Schepaschenko, D., Castanho, A., and Murdiyarso, D.: The Enduring World Forest Carbon Sink, Nature, 631, 563–569, https://doi.org/10.1038/s41586-024-07602-x, 2024.

Parisi, F., Pioli, S., Lombardi, F., Fravolini, G., Marchetti, M., and Tognetti, R.: Linking Deadwood Traits with Saproxylic Invertebrates and Fungi in European Forests – a Review, iForest, 11, 423–436, https://doi.org/10.3832/ifor2670-011, 2018.

Pastorello, G., Trotta, C., Canfora, E., Chu, H., Christianson, D., Cheah, Y. W., Poindexter, C., Chen, J., Elbashandy, A., Humphrey, M., Isaac, P., Polidori, D., Reichstein, M., Ribeca, A., van Ingen, C., Vuichard, N., Zhang, L., Amiro, B., Ammann, C., Arain, M. A., Ardo, J., Arkebauer, T., Arndt, S. K., Arriga, N., Aubinet, M., Aurela, M., Baldocchi, D., Barr, A., Beamesderfer, E., Marchesini, L. B., Bergeron, O., Beringer, J., Bernhofer, C., Berveiller, D., Billesbach, D., Black, T. A., Blanken, P. D., Bohrer, G., Boike, J., Bolstad, P. V., Bonal, D., Bonnefond, J. M., Bowling, D. R., Bracho, R., Brodeur, J., Brummer, C., Buchmann, N., Burban, B., Burns, S. P., Buysse, P., Cale, P., Cavagna, M., Cellier, P., Chen, S., Chini, I., Christensen, T. R., Cleverly, J., Collalti, A., Consalvo, C., Cook, B. D., Cook, D., Coursolle, C., Cremonese, E., Curtis, P. S., D'Andrea, E., da Rocha, H., Dai, X., Davis, K. J., Cinti, B., Grandcourt, A., Ligne, A., De Oliveira, R. C., Delpierre, N., Desai, A. R., Di Bella, C. M., Tommasi, P. D., Dolman, H., Domingo, F., Dong, G., Dore, S., Duce, P., Dufrene, E., Dunn, A., Dusek, J., Eamus, D., Eichelmann, U., ElKhidir, H. A. M., Eugster, W., Ewenz, C. M., Ewers, B., Famulari, D., Fares, S., Feigenwinter, I., Feitz, A., Fensholt, R., Filippa, G., Fischer, M., Frank, J., Galvagno, M., Gharun, M., Gianelle, D., Gielen, B., Gioli, B., Gitelson, A., Goded, I., Goeckede, M., Goldstein, A. H., Gough, C. M., Goulden, M. L., Graf, A., Griebel, A., Gruening, C., Grunwald, T., Hammerle, A., Han, S., Han, X., Hansen, B. U., Hanson, C., Hatakka, J., He, Y., Hehn, M., Heinesch, B., Hinko-Najera, N., Hortnagl, L., Hutley, L., Ibrom, A., Ikawa, H., Jackowicz-Korczynski, M., Janous, D., Jans, W., Jassal, R., Jiang, S., Kato, T., Khomik, M., Klatt, J., Knohl, A., Knox, S., Kobayashi, H., Koerber, G., Kolle, O., Kosugi, Y., Kotani, A., Kowalski, A., Kruijt, B., Kurbatova, J., Kutsch, W. L., Kwon, H., Launiainen, S., Laurila, T., Law, B., Leuning, R., Li, Y., Liddell, M., Limousin, J. M., Lion, M., Liska, A. J., Lohila, A., Lopez-Ballesteros, A., Lopez-Blanco, E., Loubet, B., Loustau, D., Lucas-Moffat, A., Luers, J., Ma, S., Macfarlane, C., Magliulo, V., Maier, R., Mammarella, I., Manca, G., Marcolla, B., Margolis, H. A., Marras, S., Massman, W., Mastepanov, M., Matamala, R., Matthes, J. H., Mazzenga, F., McCaughey, H., McHugh, I., McMillan, A. M. S., Merbold, L., Meyer, W., Meyers, T., Miller, S. D., Minerbi, S., Moderow, U., Monson, R. K., Montagnani, L., Moore, C. E., Moors, E., Moreaux, V., Moureaux, C., Munger, J. W., Nakai, T., Neirynck, J., Nesic, Z., Nicolini, G., Noormets, A., Northwood, M., Nosetto, M., Nouvellon, Y., Novick, K., Oechel, W., Olesen, J. E., Ourcival, J. M., Papuga, S. A., Parmentier, F. J., Paul-Limoges, E., Pavelka, M., Peichl, M., Pendall, E., Phillips, R. P., Pilegaard, K., Pirk, N., Posse, G., Powell, T., Prasse, H., Prober, S. M., Rambal, S., Rannik, U., Raz-Yaseef, N., Rebmann, C., Reed, D.,

Dios, V. R., Restrepo-Coupe, N., Reverter, B. R., Roland, M., Sabbatini, S., Sachs, T., Saleska, S. R., Sanchez-Canete, E. P., Sanchez-Mejia, Z. M., Schmid, H. P., Schmidt, M., Schneider, K., Schrader, F., Schroder, I., Scott, R. L., Sedlak, P., Serrano-Ortiz, P., Shao, C., Shi, P., Shironya, I., Siebicke, L., Sigut, L., Silberstein, R., Sirca, C., Spano, D., Steinbrecher, R., Stevens, R. M., Sturtevant, C., Suyker, A., Tagesson, T., Takanashi, S., Tang, Y., Tapper, N., Thom, J., Tomassucci, M., Tuovinen, J. P., Urbanski, S., Valentini, R., van der Molen, M., van Gorsel, E., van Huissteden, K., Varlagin, A., Verfaillie, J., Vesala, T., Vincke, C., Vitale, D., Vygodskaya, N., Walker, J. P., Walter-Shea, E., Wang, H., Weber, R., Westermann, S., Wille, C., Wofsy, S., Wohlfahrt, G., Wolf, S., Woodgate, W., Li, Y., Zampedri, R., Zhang, J., Zhou, G., Zona, D., Agarwal, D., Biraud, S., Torn, M., and Papale, D.: The Fluxnet2015 Dataset and the Oneflux Processing Pipeline for Eddy Covariance Data, Sci. Data, 7, 225, https://doi.org/10.1038/s41597-020-0534-3, 2020.

Pearson, T. R. H., Brown, S., Murray, L., and Sidman, G.: Greenhouse Gas Emissions from Tropical Forest Degradation: An Underestimated Source, Carbon Balance Manag., 12, 3, https://doi.org/10.1186/s13021-017-0072-2, 2017.

Pei, Y., Dong, J., Zhang, Y., Yuan, W., Doughty, R., Yang, J., Zhou, D., Zhang, L., and Xiao, X.: Evolution of Light Use Efficiency Models: Improvement, Uncertainties, and Implications, Agr. Forest Meteorol., 317, 108905, https://doi.org/10.1016/j.agrformet.2022.108905, 2022.

Phompila, C., Lewis, M., Clarke, K., and Ostendorf, B.: Monitoring Expansion of Plantations in Lao Tropical Forests Using Landsat Time Series, Land Surface Remote Sensing II, 296–306, https://doi.org/10.1117/12.2068283, 2014.

Pickering, B. J., Duff, T. J., Baillie, C., and Cawson, J. G.: Darker, Cooler, Wetter: Forest Understories Influence Surface Fuel Moisture, Agr. Forest Meteorol., 300, 108311, https://doi.org/10.1016/j.agrformet.2020.108311, 2021.

Poorter, L.: Functional Recovery of Secondary Tropical Forests (V1), DANS Data Station Life Sciences [data set], https://doi.org/10.17026/dans-zz5-hf3s, 2021.

R Core Team: R: A Language and Environment for Statistical Computing, R Foundation for Statistical Computing, Vienna, Austria, https://www.R-project.org/, 2023.

Rawat, M., Arunachalam, K., Arunachalam, A., Alatalo, J. M., and Pandey, R.: Assessment of Leaf Morphological, Physiological, Chemical and Stoichiometry Functional Traits for Understanding the Functioning of Himalayan Temperate Forest Ecosystem, Scientific Reports, 11, 23807, https://doi.org/10.1038/s41598-021-03235-6, 2021.

Reich, P. B., Uhl, C., Walters, M. B., and Ellsworth, D. S.: Leaf Lifespan as a Determinant of Leaf Structure and Function among 23 Amazonian Tree Species, Oecologia, 86, 16–24, https://doi.org/10.1007/BF00317383, 1991.

Reyes, G., Brown, S., Chapman, J., and Lugo, A. E.: Wood Densities of Tropical Tree Species, U.S. Department of Agriculture, Forest Service, Southern Forest Experiment Station, https://doi.org/10.2737/so-gtr-88, 1992.

Rodell, M., Houser, P. R., Jambor, U., Gottschalck, J., Mitchell, K., Meng, C. J., Arsenault, K., Cosgrove, B., Radakovich, J., Bosilovich, M., Entin, J. K., Walker, J. P., Lohmann, D., and Toll, D.: The Global Land Data Assimilation System, B. Am. Meteorol. Soc., 85, 381–394, https://doi.org/10.1175/BAMS-85-3-381, 2004.

Román-Dañobeytia, F. J., Levy-Tacher, S. I., Macario-Mendoza, P., and Zúñiga-Morales, J.: Redefining Secondary Forests in the Mexican Forest Code: Implications for Management, Restoration, and Conservation, MDPI journal Forests, 5, 978–991, https://doi.org/10.3390/f5050978, 2014.

Rosa, M., Rubio Neto, A., Marques, V. d. O., Silva, F. G., de Assis, E. S., Costa, A. C., Dantas, L. A., and Pereira, P. S.: Variations in Photon Flux Density Alter the Morphophysiological and Chemical Characteristics of *Anacardium Othonianum* Rizz. in Vitro, Plant Cell Tiss. Org., 140, 523–537, https://doi.org/10.1007/s11240-019-01744-x, 2020.

Rundel, P. W.: Forest Habitats and Flora in Lao Pdr, Cambodia, and Vietnam, Hanoi: WWF Indochina Programme, 171 pp., 1999.

Saner, P., Loh, Y. Y., Ong, R. C., and Hector, A.: Carbon Stocks and Fluxes in Tropical Lowland Dipterocarp Rainforests in Sabah, Malaysian Borneo, PLOS ONE, 7, e29642, https://doi.org/10.1371/journal.pone.0029642, 2012.

Santopuoli, G., Temperli, C., Alberdi, I., Barbeito, I., Bosela, M., Bottero, A., Klopčič, M., Lesinski, J., Panzacchi, P., and Tognetti, R.: Pan-European Sustainable Forest Management Indicators for Assessing Climate-Smart Forestry in Europe, Can. J. Forest Res., 51, 1741–1750, https://doi.org/10.1139/cjfr-2020-0166, 2021.

Schindelin, J., Arganda-Carreras, I., Frise, E., Kaynig, V., Longair, M., Pietzsch, T., Preibisch, S., Rueden, C., Saalfeld, S., Schmid, B., Tinevez, J. Y., White, D. J., Hartenstein, V., Eliceiri, K., Tomancak, P., and Cardona, A.: Fiji: An Open-Source Platform for Biological-Image Analysis, Nat. Methods, 9, 676–682, https://doi.org/10.1038/nmeth.2019, 2012.

Schneider, C. A., Rasband, W. S., and Eliceiri, K. W.: Nih Image to Imagej: 25 Years of Image Analysis, Nat. Methods, 9, 671–675, https://doi.org/10.1038/nmeth.2089, 2012.

Senf, C., Mori, A. S., Müller, J., and Seidl, R.: The Response of Canopy Height Diversity to Natural Disturbances in Two Temperate Forest Landscapes, Landscape Ecol., 35, 2101–2112, https://doi.org/10.1007/s10980-020-01085-7, 2020.

Senior, R. A., Hill, J. K., Benedick, S., and Edwards, D. P.: Tropical Forests Are Thermally Buffered Despite Intensive Selective Logging, Glob. Change Biol., 24, 1267–1278, https://doi.org/10.1111/gcb.13914, 2018.

Senna, M. C. A., Costa, M. H., and Shimabukuro, Y. E.: Fraction of Photosynthetically Active Radiation Absorbed by Amazon Tropical Forest: A Comparison of Field Measurements, Modeling, and Remote Sensing, J. Geophys. Res.-Biogeo., 110, G01008, https://doi.org/10.1029/2004JG000005, 2005.

Shannon, C. E.: A Mathematical Theory of Communication, Bell Syst. Tech. J., 27, 379–423, https://doi.org/10.1002/j.1538-7305.1948.tb01338.x, 1948.

Shannon, V. L., Vanguelova, E. I., Morison, J. I. L., Shaw, L. J., and Clark, J. M.: The Contribution of Deadwood to Soil Carbon Dynamics in Contrasting Temperate Forest Ecosystems, Eur. J. For. Res., 141, 241–252, https://doi.org/10.1007/s10342-021-01435-3, 2021.

Slik, J. W. F., Aiba, S. I., Brearley, F. Q., Cannon, C. H., Forshed, O., Kitayama, K., Nagamasu, H., Nilus, R., Payne, J., Paoli, G., Poulsen, A. D., Raes, N., Sheil, D., Sidiyasa, K., Suzuki, E., and van Valkenburg, J. L. C. H.: Environmental Correlates of Tree Biomass, Basal Area, Wood Specific Gravity and Stem Density

Gradients in Borneo's Tropical Forests, Global Ecol. Biogeogr., 19, 50–60, https://doi.org/10.1111/j.1466-8238.2009.00489.x, 2010.

Sodhi, N. S., Koh, L. P., Brook, B. W., and Ng, P. K.: Southeast Asian Biodiversity: An Impending Disaster, Trends Ecol. Evol., 19, 654–660, https://doi.org/10.1016/j.tree.2004.09.006, 2004.

Sola, G., Vanna, S., Vesa, L., Van Rijn, M., and Henry, M.: Forest Biomass in Cambodia: from Field Plot to National Estimates, UN-REDD Programme, Phnom Penh, Cambodia, https://cambodia-redd.org/wp-content/uploads/2016/01/Forest-biomass-in-Cambodia-from-field-plots-to-national-estimates.pdf, 2014.

Somaly, O., Sasaki, N., Kimchhin, S., Tsusaka, T. W., Shrestha, S., and Malyne, N.: Impact of Forest Cover Change in Phnom Kulen National Park on Downstream Local Livelihoods Along Siem Reap River, Cambodia, International Journal of Environmental and Rural Development, 11, 93–99, https://doi.org/10.32115/ijerd.11.1_93, 2020.

Sovann, C., Tagesson, T., Kok, S., and Olin, S.: Forest Inventory, Leaf Area Index, and Leaf Functional Traits of Various Land Cover Classes in Kulen, Cambodia, Zenodo [data set], https://doi.org/10.5281/zenodo.10146582, 2024a.

Sovann, C., Tagesson, T., Vestin, P., Kok, S., and Olin, S.: Daily Fraction of Photosynthetically Active Radiation (Fpar), Edaphic, and Weather Conditions from 20220410 to 20230409 in Kulen, Cambodia, Zenodo [data set], https://doi.org/10.5281/zenodo.10159726, 2024b.

Sovann, C., Tagesson, T., Vestin, P., Kok, S., and Olin, S.: Weather Conditions from 20220410 to 20240409 in Kulen, Cambodia, Zenodo [dataset], https://doi.org/10.5281/zenodo.13756906, 2024c.

Sovann, C., Olin, S., Mansourian, A., Sakhoeun, S., Prey, S., Kok, S., and Tagesson, T.: Importance of Spectral Information, Seasonality, and Topography on Land Cover Classification of Tropical Land Cover Mapping, Remote Sens., 17, 1551, https://doi.org/10.3390/rs17091551, 2025.

Sovu, Tigabu, M., Savadogo, P., Odén, P. C., and Xayvongsa, L.: Recovery of Secondary Forests on Swidden Cultivation Fallows in Laos, Forest Ecol. Manag., 258, 2666–2675, https://doi.org/10.1016/j.foreco.2009.09.030, 2009.

Steur, G., Ter Steege, H., Verburg, R. W., Sabatier, D., Molino, J. F., Banki, O. S., Castellanos, H., Stropp, J., Fonty, E., Ruysschaert, S., Galbraith, D., Kalamandeen, M., van Andel, T. R., Brienen, R., Phillips, O. L., Feeley, K. J., Terborgh, J., and Verweij, P. A.: Relationships between Species Richness and Ecosystem Services in Amazonian Forests Strongly Influenced by Biogeographical Strata and Forest Types, Sci. Rep., 12, 5960, https://doi.org/10.1038/s41598-022-09786-6, 2022.

Stibig, H.-J., Achard, F., Carboni, S., Raši, R., and Miettinen, J.: Change in tropical forest cover of Southeast Asia from 1990 to 2010, Biogeosciences, 11, 247–258, https://doi.org/10.5194/bg-11-247-2014, 2014.

Stirbet, A., Lazár, D., Guo, Y., and Govindjee, G.: Photosynthesis: Basics, History and Modelling, Annals of Botany, 126, 511–537, https://doi.org/10.1093/aob/mcz171, 2020.

Suratman, M. N.: Tree Species Diversity and Forest Stand Structure of Pahang National Park, Malaysia, in: Biodiversity Enrichment in a Diverse World, edited by: Lameed, G. A., IntechOpen, Rijeka, Croatia, 45–56, https://doi.org/10.5772/50339, 2012.

Swedish University of Agricultural Sciences: Field Work Instructions 2021, Swedish National Forest Inventory and Swedish Soil Inventory, Department of Forest Resource Management, Umeå, and Department of Soil and Environment, Uppsala, Sweden, https://www.slu.se/en/about-slu/organisation/departments/forest-resource-management/miljoanalys/nfi/about-nfi/field-instructions/ (last access: 10 September 2025), 2021.

Tang, C., Liu, Y., Li, Z., Guo, L., Xu, A., and Zhao, J.: Effectiveness of Vegetation Cover Pattern on Regulating Soil Erosion and Runoff Generation in Red Soil Environment, Southern China, Ecol. Indic., 129, 107956, https://doi.org/10.1016/j.ecolind.2021.107956, 2021.

ter Steege, H., Pitman, N. C. A., do Amaral, I. L., de Souza Coelho, L., de Almeida Matos, F. D., de Andrade Lima Filho, D., Salomão, R. P., Wittmann, F., Castilho, C. V., Guevara, J. E., Veiga Carim, M. d. J., Phillips, O. L., Magnusson, W. E., Sabatier, D., Revilla, J. D. C., Molino, J.-F., Irume, M. V., Martins, M. P., da Silva Guimarães, J. R., Ramos, J. F., Bánki, O. S., Piedade, M. T. F., Cárdenas López, D., Rodrigues, D. d. J., Demarchi, L. O., Schöngart, J., Almeida, E. J., Barbosa, L. F., Cavalheiro, L., dos Santos, M. C. V., Luize, B. G., de Leão Novo, E. M. M., Vargas, P. N., Silva, T. S. F., Venticinque, E. M., Manzatto, A. G., Reis, N. F. C., Terborgh, J., Casula, K. R., Honorio Coronado, E. N., Monteagudo Mendoza, A., Montero, J. C., Costa, F. R. C., Feldpausch, T. R., Quaresma, A. C., Castaño Arboleda, N., Zartman, C. E., Killeen, T. J., Marimon, B. S., Marimon-Junior, B. H., Vasquez, R., Mostacedo, B., Assis, R. L., Baraloto, C., do Amaral, D. D., Engel, J., Petronelli, P., Castellanos, H., de Medeiros, M. B., Simon, M. F., Andrade, A., Camargo, J. L., Laurance, W. F., Laurance, S. G. W., Maniguaje Rincón, L., Schietti, J., Sousa, T. R., de Sousa Farias, E., Lopes, M. A., Magalhães, J. L. L., Nascimento, H. E. M., de Queiroz, H. L., Aymard C, G. A., Brienen, R., Stevenson, P. R., Araujo-Murakami, A., Baker, T. R., Cintra, B. B. L., Feitosa, Y. O., Mogollón, H. F., Duivenvoorden, J. F., Peres, C. A., Silman, M. R., Ferreira, L. V., Lozada, J. R., Comiskey, J. A., Draper, F. C., de Toledo, J. J., Damasco, G., García-Villacorta, R., Lopes, A., Vicentini, A., Cornejo Valverde, F., Alonso, A., Arroyo, L., Dallmeier, F., Gomes, V. H. F., Jimenez, E. M., Neill, D., Peñuela Mora, M. C., Noronha, J. C., de Aguiar, D. P. P., Barbosa, F. R., Bredin, Y. K., de Sá Carpanedo, R., Carvalho, F. A., de Souza, F. C., Feeley, K. J., Gribel, R., Haugaasen, T., Hawes, J. E., Pansonato, M. P., Ríos Paredes, M., Barlow, J., Berenguer, E., da Silva, I. B., Ferreira, M. J., Ferreira, J., Fine, P. V. A., Guedes, M. C., Levis, C., Licona, J. C., Villa Zegarra, B. E., Vos, V. A., Cerón, C., Durgante, F. M., Fonty, É., Henkel, T. W., Householder, J. E., Huamantupa-Chuquimaco, I., Pos, E., Silveira, M., Stropp, J., Thomas, R., Daly, D., Dexter, K. G., Milliken, W., Molina, G. P., Pennington, T., Vieira, I. C. G., Weiss Albuquerque, B., Campelo, W., Fuentes, A., Klitgaard, B., Pena, J. L. M., Tello, J. S., Vriesendorp, C., Chave, J., Di Fiore, A., Hilário, R. R., de Oliveira Pereira, L., Phillips, J. F., Rivas-Torres, G., van Andel, T. R., von Hildebrand, P., Balee, W., Barbosa, E. M., de Matos Bonates, L. C., Dávila Doza, H. P., Zárate Gómez, R., Gonzales, T., Gallardo Gonzales, G. P., Hoffman, B., Junqueira, A. B., Malhi, Y., de Andrade Miranda, I. P., Pinto, L. F. M., Prieto, A., Rudas, A., Ruschel, A. R., Silva, N., Vela, C. I. A., Zent, E. L., Zent, S., Cano, A., Carrero Márquez, Y. A., Correa,

D. F., Costa, J. B. P., Flores, B. M., Galbraith, D., Holmgren, M., Kalamandeen, M., Lobo, G., Torres Montenegro, L., Nascimento, M. T., Oliveira, A. A., Pombo, M. M., Ramirez-Angulo, H., Rocha, M., Scudeller, V. V., Sierra, R., Tirado, M., Umaña, M. N., van der Heijden, G., Vilanova Torre, E., Reategui, M. A. A., Baider, C., Balslev, H., Cárdenas, S., Casas, L. F., Endara, M. J., Farfan-Rios, W., Ferreira, C., Linares-Palomino, R., Mendoza, C., Mesones, I., Parada, G. A., Torres-Lezama, A., Urrego Giraldo, L. E., Villarroel, D., Zagt, R., Alexiades, M. N., de Oliveira, E. A., Garcia-Cabrera, K., Hernandez, L., Cuenca, W. P., Pansini, S., Pauletto, D., Ramirez Arevalo, F., Sampaio, A. F., Valderrama Sandoval, E. H., Gamarra, L. V., Levesley, A., Pickavance, G., and Melgaço, K.: Mapping Density, Diversity and Species-Richness of the Amazon Tree Flora, Communications Biology, 6, 1130, https://doi.org/10.1038/s42003-023-05514-6, 2023.

Than, S., Vesa, L., Vanna, S., Hyvönen, P., Korhonen, K., Gael, S., Matieu, H., and van Rijn, M.: Field Manual for the National Forest Inventory of Cambodia, 2nd edn., Forest Administration of the Ministry of Agriculture, Forestry and Fisheries & Food and Agriculture Organization of the United Nations, Phnom Penh, Cambodia, 2018.

Theilade, I., Phourin, C., Schmidt, L., Meilby, H., Van De Bult, M., and Friborg, K. G.: Evergreen Forest Types of the Central Plains in Cambodia: Floristic Composition and Ecological Characteristics, Nord. J. Bot., 2022, e03494, https://doi.org/10.1111/njb.03494, 2022.

Thiel, S., Tschapka, M., Heymann, E. W., and Heer, K.: Vertical Stratification of Seed-Dispersing Vertebrate Communities and Their Interactions with Plants in Tropical Forests, Biol. Rev., 96, 454–469, https://doi.org/10.1111/brv.12664, 2021.

Tilman, D., Lehman, C. L., and Thomson, K. T.: Plant Diversity and Ecosystem Productivity: Theoretical Considerations, P. Natl. Acad. Sci. USA, 94, 1857–1861, https://doi.org/10.1073/pnas.94.5.1857, 1997.

Tito, R., Salinas, N., Cosio, E. G., Espinoza, T. E. B., Muñiz, J. G., Aragón, S., Nina, A., and Roman-Cuesta, R. M.: Secondary Forests in Peru: Differential Provision of Ecosystem Services Compared to Other Post-Deforestation Forest Transitions, Ecol. Soc., 27, 12, https://doi.org/10.5751/Es-13446-270312, 2022.

Tláskal, V., Brabcová, V., Větrovský, T., Jomura, M., López-Mondéjar, R., Monteiro, L. M. O., Saraiva, J. P., Human, Z. R., Cajthaml, T., Rocha, U. N. d., and Baldrian, P.: Complementary Roles of Wood-Inhabiting Fungi and Bacteria Facilitate Deadwood Decomposition, 6, https://doi.org/10.1128/msystems.01078-20, 2021.

Townsend, A. R., Cleveland, C. C., Houlton, B. Z., Alden, C. B., and White, J. W. C.: Multi-Element Regulation of the Tropical Forest Carbon Cycle, Front. Ecol. Environ., 9, 9–17, https://doi.org/10.1890/100047, 2011.

Tynsong, H., Dkhar, M., and Tiwari, B. K.: Tree Diversity and Vegetation Structure of the Tropical Evergreen Forests of the Southern Slopes of Meghalaya, North East India, Asian Journal of Forestry, 6, 22–33, https://doi.org/10.13057/asianjfor/r060104, 2022.

Van Do, T., Yamamoto, M., Kozan, O., Hai, V. D., Trung, P. D., Thang, N. T., Hai, L. T., Nam, V. T., Hung, T. T., Van Thang, H., Manh, T. D., Khiem, C. C., Lam, V. T., Hung, N. Q., Quy, T. H., Tuyen, P. Q., Bon, T. N., Phuong, N. T. T., Khuong, N. V., Van Tuan, N., Ha, D. T. H., Long, T. H., Van Thuyet, D., Trieu, D. T., Van Thinh, N., Hai, T. A., Trung, D. Q., Van Bich, N., Dang, D. H., Dung, P. T., Hoang, N. H., Hanh, L. T., Quang, P. M., Huong, N. T. T., Son, H. T., Son, N. T., Van Anh, N. T., Anh, N. T. H., Sam, P. D., Nhung, H. T., Van Thanh, H., Thinh, N. H., Van, T. H., Luong, H. T., and Hung, B. K.: Ecoregional Variations of Aboveground Biomass and Stand Structure in Evergreen Broadleaved Forests, J. Forestry Res., 31, 1713–1722, https://doi.org/10.1007/s11676-019-00969-y, 2019.

van Galen, L. G., Jordan, G. J., and Baker, S. C.: Relationships between Coarse Woody Debris Habitat Quality and Forest Maturity Attributes, Conservation Science and Practice, 1, e55, https://doi.org/10.1111/csp2.55, 2019.

van Haren, J., de Oliveira Jr., R. C., Beldini, P. T., de Camargo, P. B., Keller, M., and Saleska, S.: Tree Species Effects on Soil Properties and Greenhouse Gas Fluxes in East-Central Amazonia: Comparison between Monoculture and Diverse Forest, Biotropica, 45, 709–718, https://doi.org/10.1111/btp.12061, 2013.

Van, Y. T. and Cochard, R.: Tree Species Diversity and Utilities in a Contracting Lowland Hillside Rainforest Fragment in Central Vietnam, Forest Ecosystems, 4, 9, https://doi.org/10.1186/s40663-017-0095-x, 2017.

Vestin, P., Mölder, M., Kljun, N., Cai, Z., Hasan, A., Holst, J., Klemedtsson, L., and Lindroth, A.: Impacts of Clear-Cutting of a Boreal Forest on Carbon Dioxide, Methane and Nitrous Oxide Fluxes, Forests, 11, 961, https://doi.org/10.3390/f11090961, 2020.

Victor, A. D., Valery, N. N., Boris, N., Aimé, V. B. T., and Louis, Z.: Carbon Storage in Cashew Plantations in Central Africa: Case of Cameroon, Carbon Manag., 12, 25–35, https://www.tandfonline.com/doi/citedby/10.1080/17583004.2020.1858682, 2021.

Vieilledent, G., Vaudry, R., Andriamanohisoa, S. F. D., Rakotonarivo, O. S., Randrianasolo, H. Z., Razafindrabe, H. N., Rakotoarivony, C. B., Ebeling, J., and Rasamoelina, M.: A Universal Approach to Estimate Biomass and Carbon Stock in Tropical Forests Using Generic Allometric Models, Ecol. Appl., 22, 572–583, https://doi.org/10.1890/11-0039.1, 2012.

Waide, R. B., Willig, M. R., Steiner, C. F., Mittelbach, G., Gough, L., Dodson, S. I., Juday, G. P., and Parmenter, R.: The Relationship between Productivity and Species Richness, Annu. Rev. Ecol. Syst., 30, 257–300, https://doi.org/10.1146/annurev.ecolsys.30.1.257, 1999.

Wang, P., Li, R., Liu, D., and Wu, Y.: Dynamic Characteristics and Responses of Ecosystem Services under Land Use/Land Cover Change Scenarios in the Huangshui River Basin, China, Ecol. Indic., 144, 109539, https://doi.org/10.1016/j.ecolind.2022.109539, 2022.

Wang, R., Yu, G., He, N., Wang, Q., Zhao, N., and Xu, Z.: Latitudinal Variation of Leaf Morphological Traits from Species to Communities Along a Forest Transect in Eastern China, J. Geogr. Sci., 26, 15–26, https://doi.org/10.1007/s11442-016-1251-x, 2016.

Wang, S., Fu, B. J., Gao, G. Y., Yao, X. L., and Zhou, J.: Soil moisture and evapotranspiration of different land cover types in the Loess Plateau, China, Hydrol. Earth Syst. Sci., 16, 2883–2892, https://doi.org/10.5194/hess-16-2883-2012, 2012.

Wang, W., Liu, H. M., Zhang, J. H., Li, Z. Y., Wang, L. X., Wang, Z., Wu, Y. T., Wang, Y., and Liang, C. Z.: Effect of Grazing Types on Community-Weighted Mean Functional Traits and Ecosystem

Functions on Inner Mongolian Steppe, China, Sustainability, 12, 7169, https://doi.org/10.3390/su12177169, 2020.

West, G. B. and Brown, J. H.: The Origin of Allometric Scaling Laws in Biology from Genomes to Ecosystems: Towards a Quantitative Unifying Theory of Biological Structure and Organization, J. Exp. Biol., 208, 1575–1592, https://doi.org/10.1242/jeb.01589, 2005.

Whitmore, T. C.: An Introduction to Tropical Forests, 2nd edn., Oxford University Press, Oxford, England, ISBN 9780198501480, 1998.

Woodall, C. W., Evans, D. M., Fraver, S., Green, M. B., Lutz, D. A., and D'Amato, A. W.: Real-Time Monitoring of Deadwood Moisture in Forests: Lessons Learned from an Intensive Case Study, Can. J. Forest Res., 50, 1244–1252, https://doi.org/10.1139/cjfr-2020-0110, 2020.

Wright, I. J., Reich, P. B., Westoby, M., Ackerly, D. D., Baruch, Z., Bongers, F., Cavender-Bares, J., Chapin, T., Cornelissen, J. H., Diemer, M., Flexas, J., Garnier, E., Groom, P. K., Gulias, J., Hikosaka, K., Lamont, B. B., Lee, T., Lee, W., Lusk, C., Midgley, J. J., Navas, M. L., Niinemets, U., Oleksyn, J., Osada, N., Poorter, H., Poot, P., Prior, L., Pyankov, V. I., Roumet, C., Thomas, S. C., Tjoelker, M. G., Veneklaas, E. J., and Villar, R.: The Worldwide Leaf Economics Spectrum, Nature, 428, 821–827, https://doi.org/10.1038/nature02403, 2004.

Wright, S. J.: The Carbon Sink in Intact Tropical Forests, Glob. Change Biol., 19, 337–339, https://doi.org/10.1111/gcb.12052, 2013.

Xiao, Z. Q., Liang, S. L., Sun, R., Wang, J. D., and Jiang, B.: Estimating the Fraction of Absorbed Photosynthetically Active Radiation from the Modis Data Based Glass Leaf Area Index Product, Remote Sens. Environ., 171, 105–117, https://doi.org/10.1016/j.rse.2015.10.016, 2015.

Yen, V. T. and Cochard, R.: Chapter 5 – Structure and Diversity of a Lowland Tropical Forest in Thua Thien Hue Province, in: Redefining Diversity & Dynamics of Natural Resources Management in Asia, Volume 3, edited by: Thang, T. N., Dung, N. T., Hulse, D., Sharma, S., and Shivakoti, G. P., Elsevier, 71–85, https://doi.org/10.1016/B978-0-12-805452-9.00005-9, 2017.

Zanne, A. E., Lopez-Gonzalez, G., Coomes, D. A., Ilic, J., Jansen, S., Lewis, S. L., Miller, R. B., Swenson, N. G., Wiemann, M. C., and Chave, J.: Data From: Towards a Worldwide Wood Economics Spectrum, DRYAD [data set], https://doi.org/10.5061/dryad.234, 2009.

Zhang, P., Hefting, M. M., Soons, M. B., Kowalchuk, G. A., Rees, M., Hector, A., Turnbull, L. A., Zhou, X., Guo, Z., Chu, C., Du, G., and Hautier, Y.: Fast and Furious: Early Differences in Growth Rate Drive Short-Term Plant Dominance and Exclusion under Eutrophication, Ecol. Evol., 10, 10116–10129, https://doi.org/10.1002/ece3.6673, 2020.

Zhao, W., Tan, W., and Li, S.: High Leaf Area Index Inhibits Net Primary Production in Global Temperate Forest Ecosystems, Environ. Sci. Pollut. Res. Int., 28, 22602–22611, https://doi.org/10.1007/s11356-020-11928-0, 2021.

Ziegler, S. S.: A Comparison of Structural Characteristics between Old-Growth and Postfire Second-Growth Hemlock–Hardwood Forests in Adirondack Park, New York, U. S. A, Global Ecol. Biogeogr., 9, 373–389, https://doi.org/10.1046/j.1365-2699.2000.00191.x, 2000.

Zin, I. I. S. and Mitlöhner, R.: Species Composition and Stand Structure of Primary and Secondary Moist Evergreen Forests in the Tanintharyi Nature Reserve (Tnr) Buffer Zone, Myanmar, Open Journal of Forestry, 10, 445–459, https://doi.org/10.4236/ojf.2020.104028 2020.